

**Development of Thermoplastic 3D Woven Composite**

by

Kang Chin Ann

24059

Dissertation submitted in partial fulfilment of  
the requirements for the  
Bachelor of Mechanical Engineering with Honours

JANUARY 2020

Universiti Teknologi PETRONAS

Bandar Seri Iskandar

32610 Seri Iskandar

Perak Darul Ridzuan

# **CERTIFICATION OF APPROVAL**

**Development of Thermoplastic 3D Woven Composite**

by

**KANG CHIN ANN**

24059

A project dissertation submitted to the

Mechanical Engineering Programme

Universiti Teknologi PETRONAS

in partial fulfilment of the requirement for the

**BACHELOR OF MECHANICAL ENGINEERING WITH HONOURS**

Approved by,

*puteri megat*

.....

**ASSOC PROF. DR. PUTERI SRI MELOR BINTI MEGAT YUSOFF**

**UNIVERSITI TEKNOLOGI PETRONAS**

**TRONOH, PERAK**

**JANUARY 2020**

## **CERTIFICATION OF ORIGINALITY**

This is to clarify that I am responsible for the work submitted in this project, that the original work is my own except as specified in the references and acknowledgements, and that the original work contained herein have not been undertaken or done by unspecified sources or persons.

A handwritten signature in black ink, appearing to read 'Kang Chin Ann', written in a cursive style. The signature is positioned above a horizontal dotted line.

**KANG CHIN ANN**

## ABSTRACT

There is a growing concern over the recycling issue of thermosetting composite and the weakness of 2D composite in resisting out-of-plane load in composite manufacturing industry. In this paper, the effect of the off-axis angle on the flexural behaviours of thermosetting and thermoplastic three-dimensional woven composites will be presented and the suitability of thermoplastic 3D woven composite as a substituent for thermosetting 3D woven composite will be assessed. Three-point bending test is employed to test six kinds of samples made of thermoplastics and thermosetting resins at 0 degree, 45 degree and 90 degree. Visual inspection is carried out on the damaged samples to characterise the macro-scale damage of 3D woven composite fractured in bending. Besides, numerical analysis is performed as an attempt to replace the role of experiment in predicting the flexural strength of both thermosetting and thermoplastic at various off-axis angles. Experimental results show that there are merely minor differences between thermoplastic and thermosetting 3D woven composite samples in terms of flexural properties at all tested angles. Simulation is proven as a viable way to show the trend of the flexural strength as off-axis angle changes. However, numerical results do not really agree with experimental results as modelling is conducted at macro-scale level. As an improvement, reduction of voids, modelling at macro-scale level and micro-scale damage characterisation are suggested as future work.

*Keywords:* Thermoplastic, thermoset, 3D woven composite, flexural properties, off-axis angle, numerical analysis

## **ACKNOWLEDGEMENT**

First, I am grateful towards my FYP supervisor, AP. Dr. Puteri Sri Melor Binti Megat Yusoff for all the guidance she has offered me throughout the seven months of undertaking FYP. She has always been very efficient at replying my email asking for feedbacks on my FYP reports and presentation slides. Besides, she never rejects my request to have meeting with her to discuss FYP related issues despite her hectic schedules as the head of department for mechanical engineering.

Furthermore, I would like to express my greatest gratitude to Mr. Shah Syed Zulfiqar Hussain who has been very helpful in every aspect of this project. Not only has he shown me the step for vacuum infusion process and three-point bending test, he has guided me step by step to run the simulation using ABAQUS software. More importantly, he has provided essential data on the mechanical properties of thermosetting and thermosetting 3D woven as an input data for finite element analysis. Without his continuous support, this project would not have been so successful.

Besides, my friends and families should not be forgotten for they being really supportive throughout my period of ups and downs in completing my FYP.

# TABLE OF CONTENTS

<b>CERTIFICATION OF APPROVAL</b> .....	i
<b>CERTIFICATION OF ORIGINALITY</b> .....	ii
<b>ABSTRACT</b> .....	iii
<b>ACKNOWLEDGEMENT</b> .....	iv
<b>LIST OF FIGURES</b> .....	vii-viii
<b>LIST OF TABLES</b> .....	ix
<b>NOMENCLATURE</b> .....	x
<b>CHAPTER 1: INTRODUCTION</b>	
1.1 Background of Study.....	1-2
1.2 Problem Statement.....	2-3
1.3 Objectives.....	3
1.4 Scope of Study.....	4
<b>CHAPTER 2: LITERATURE REVIEW</b>	
2.1 Resin Matrix.....	5-6
2.2 Flexural Properties of 3D Composite.....	6-11
2.3 Damage Mode of 3D Composite.....	11-14
<b>CHAPTER 3: METHODOLOGY</b>	
3.1 Project Activities.....	15
3.2 Vacuum Infusion Process.....	16
3.3 Three-point Bending Test.....	16-18
3.4 Finite Element Analysis.....	18-21
3.5 Gantt Chart.....	22
3.6 Project Key Milestones.....	23

## **CHAPTER 4: RESULTS AND DISCUSSIONS**

4.1	Three-point Bending Test .....	24-29
4.2	Macro-scale Damage Characterisation.....	29-31
4.3	ABAQUS Simulation.....	31-41

## **CHAPTER 5: CONCLUSION AND RECOMMENDATION**

5.1	Conclusion.....	42-43
5.2	Recommendation.....	43

<b>REFERENCES</b> .....	44-46
-------------------------	-------

## LIST OF FIGURES

Figure 1.1: Architecture of 3D orthogonal woven fabric with plain weave and 4 layers.....	2
Figure 2.1: Comparison of thermoset and thermoplastic polymer structures.....	6
Figure 2.2: Typical flexural test curves.....	7
Figure 2.3: Maximum stress of four kinds of angle samples.....	8
Figure 2.4: Variation in flexural strength.....	10
Figure 2.5: Typical morphologies of bending failure for different z-binder volume fraction.....	11
Figure 2.6: XCT scans of front and side of samples tested after flexural tests (a, b) orthogonal, (c, d) angle interlock, and (e, f) layer to layer.....	12
Figure 2.7: Failure mode after 3-point bending test (left: 3D composite; right: 2D composite). (a) front surface; (b) rear surface.....	13
Figure 2.8: Macro failure modes of 0 degree sample (a), 30 degrees sample (b), 45 degrees sample (c) and 90 degrees sample (d).....	14
Figure 3.1: Project Workflow.....	15
Figure 3.2: Setup for vacuum infusion process.....	16
Figure 3.3: Three-point Loading Configuration with Fixed Supports and Loading Nose.....	17
Figure 3.4: Setup of three-point bending load in simulation.....	18
Figure 3.5: Simulation model with mesh.....	20
Figure 3.6: Interaction between loading nose and beam.....	20
Figure 4.1: Experimental flexural stress strain curve of thermosetting and thermoplastic samples.....	25
Figure 4.2: Experimental flexural strength of thermosetting and thermoplastic samples.....	26
Figure 4.3: Experimental flexural modulus of thermosetting and thermoplastic samples.....	27
Figure 4.4: Experimental flexural strain of thermosetting and thermoplastic samples.....	28
Figure 4.5: Experimental energy absorption of thermosetting and thermoplastic	



samples.....	29
Figure 4.6: Macro-scale damage on rear surfaces of on-axis samples including thermosetting 0 degree sample (a), thermosetting 90 degree sample (b), thermoplastic 0 degree sample (c), and thermoplastic 90 degree sample (d)...	30
Figure 4.7: Macro-scale damage on rear surfaces of off-axis samples including thermosetting 45 degree sample (a), and thermoplastic 45 degree sample (b).....	31
Figure 4.8: Damage initiation of 0 degree thermosetting 3D woven composite.....	36
Figure 4.9: Damage initiation of 15 degree thermosetting 3D woven composite..	36
Figure 4.10: Damage initiation of 30 degree thermosetting 3D woven composite....	36
Figure 4.11: Damage initiation of 45 degree thermosetting 3D woven composite.....	37
Figure 4.12: Damage initiation of 60 degree thermosetting 3D woven composite....	37
Figure 4.13: Damage initiation of 75 degree thermosetting 3D woven composite.....	37
Figure 4.14: Damage initiation of 90 degree thermosetting 3D woven composite....	38
Figure 4.15: Damage initiation of 0 degree thermoplastic 3D woven composite.....	38
Figure 4.16: Damage initiation of 15 degree thermoplastic 3D woven composite....	38
Figure 4.17: Damage initiation of 30 degree thermoplastic 3D woven composite.....	39
Figure 4.18: Damage initiation of 45 degree thermoplastic 3D woven composite....	39
Figure 4.19: Damage initiation of 60 degree thermoplastic 3D woven composite....	39
Figure 4.20: Damage initiation of 75 degree thermoplastic 3D woven composite....	40
Figure 4.21: Damage initiation of 90 degree thermoplastic 3D woven composite....	40
Figure 4.22: Comparison of thermoplastic and thermosetting specimens at different off-axis angles in terms of numerical flexural strength.....	40

## LIST OF TABLES

Table 2.1: Geometric data of the reinforcements.....	11
Table 3.1: Specification of samples.....	17
Table 3.2: Elastic mechanical behaviour of composites.....	19
Table 3.3: Material properties of composites for hashin damage criterion.....	19
Table 3.4: Elastic mechanical behaviour of supports and loading nose.....	19
Table 3.5: Boundary conditions on the simulation model.....	21
Table 3.6: Gannt chart.....	22
Table 3.7: Project Milestone of FYP I.....	23
Table 3.8: Project Milestone of FYP II.....	23
Table 4.1: Comparison of experimental and numerical flexural strength.....	41

## NOMENCLATURE

$E_1$	Young's modulus along x-axis
$E_2$	Young's modulus along y-axis
$E_3$	Young's modulus along z-axis
$\nu_{12}$	Poisson's ratio for xy-plane
$\nu_{13}$	Poisson's ratio for xz-plane
$\nu_{23}$	Poisson's ratio for zy-plane
$G_{12}$	Shear modulus for xy-plane
$G_{13}$	Shear modulus for xz-plane
$G_{23}$	Shear modulus for yz-plane
$T_L$	Tensile strength along longitudinal direction
$T_T$	Tensile strength along transverse direction
$C_L$	Compressive strength along longitudinal direction
$C_T$	Compressive strength along transverse direction
$S_L$	Shear strength along longitudinal direction
$S_T$	Shear strength along transverse direction

# CHAPETER 1

## INTRODUCTION

### 1.1 Background of Study

A composite material is a material made from two or more constituent materials with significantly different chemical and physical properties that can produce resulting material with enhanced properties when combined. The components of a composite can be divided into two which are fibre and resin matrix. Fibre is the component that carries most of the load exerted on the composite while resin matrix is the component that distribute the load evenly throughout the composite to prevent centralized stress from building at a particular point on the composite. Not to be confused with other mixtures and solid solutions, fibre and resin are mixed and bonded on a macroscopic scale with distinct phases having recognizable interfaces between them. When compared to conventional materials, composite can offer numerous advantages such as light weight, low material cost, design flexibility, durability, corrosion resistance and so on, gaining itself huge popularity in industries like aerospace, automotive, civil infrastructure, marine, corrosive environment and so on, just to name a few.

Traditionally, fibre reinforced composite material are produced as laminates by reinforcing matrix material by long fibres. The composites are designed by combining different fiber directions and also varying the thickness by changing the number of layers stacked on each other in order to meet the mechanical requirement. Fibre is normally oriented in the direction which bears the major stress when the composite is in service. This is because composite is an anisotropic material, causing it to have different mechanical properties along three different axes. Laminated composites have excellent in-plane strength but limited out-of-plane strength which results in weak shear strength between the laminas. Laminated composites commonly fail due to delamination because the out-of-plane strength is only provided by the matrix material and bonding materials between laminas.

The out-of-plane strength of fibre reinforced composite is then improved by introducing 3D fibre reinforcement. 3D fibre reinforced composites have advantages over laminated composites by eliminating potential dimensional variation, having

direct manufacturing of preforms and better delamination resistance. As compared to 2D fibre reinforced composites which only have yarns running in warp and weft direction, 3D fibre reinforced composites have three sets of yarns including warp yarns, weft yarns and z-yarns in three perpendicular directions. Warp yarns and weft yarns can also be named as y-yarns and x-yarns. 3D fibre reinforced composite was invented when Mohamed and Zhang patented a weaving method to produce the 3D woven fabric which was known as 3D orthogonal woven fabric [1]. In this type of 3D woven fabric, there is no interlacing between the warp yarns and the weft yarns which are perpendicular to each other instead. The warp layers and the weft layers are held in position by having the z-yarns interlacing through the thickness along the warp direction over the weft yarns. The advantage of the orthogonal structure in this type of 3D woven fabric is that the load carrying ability of the composite are optimized through the reduced crimp of warp yarns and weft yarns. The schematic diagram of 3D orthogonal woven preform with plain weave for 4 layers is shown in Figure 1.1.

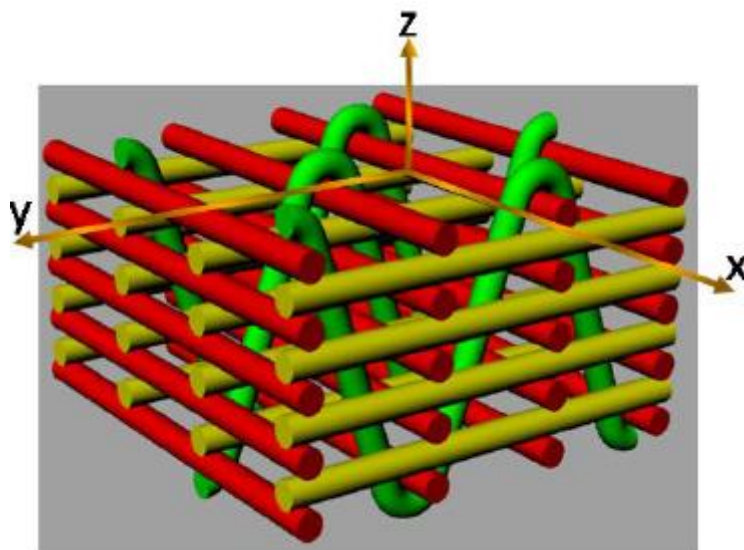


Figure 1.1: Architecture of 3D orthogonal woven fabric with plain weave and 4 layers [2]

## 1.2 Problem Statements

Unlike thermoplastics FRPs that can be easily recycled by melting and remoulding, it is difficult to recycle thermosetting FRPs due the cross-lined nature of resin matrix. Unfortunately, most of the research on composite manufacturing is geared more

towards the properties of thermosetting FRPs, leaving a big research gap on the properties of thermoplastics FRPs and causing thermosetting FRPs to be more widely used in manufacturing industries. In Portugal, the average landfill fee in 2010 was about 26 euro per tonne and this figure was estimated to increase up to 120 euros per tonne for composite wastes by the end of 2013 [3]. Besides, the incineration tax is expected to experience similar trend as landfill tax in order to encourage re-use and recycling of waste where possible before landfill and incineration. In France, the landfill tax and incineration tax for general waste in 2015 are found to be around 95 euros per tonne and 92 euros per tonne respectively [4]. From these facts, it can be inferred that FRP manufacturers gradually loses their competitiveness due to thermosetting FRP products being unrecyclable.

On the other hand, most of the composite stiffeners are made of unidirectional or 2D woven fabrics or the combination of both [5]. As a result, these stiffeners have critical pitfalls of suffering delamination at low loadings, limiting their uses where shear and transverse loads, such as in bending, are substantial. The drawback is especially conspicuous for composite structures having curvatures. When tensile and compressive bending is subjected on these structures in the plane of curvatures, radial stress will develop in the z-direction and result in premature delamination failure. On the contrary, 3D woven fabric composites with fibre in z-direction provide high through-thickness strengths, damage resistance and delamination resistance. These improvements are attributed to the presence of continuous z-direction fibres and thus it becomes urgent in bringing 3D composites into wide application, especially in making composite stiffeners.

### **1.3 Objectives**

The objectives of the project are:

- i) To investigate the flexural properties of thermoplastics and thermosetting 3D fibre reinforced composites
- ii) To assess the suitability of thermoplastics 3D woven composite as a substituent for thermosetting 3D woven composite

#### **1.4 Scope of Study**

The scope of this study is limited to determining the flexural property of thermoplastics and thermosetting 3D woven composite through three-point bending test. The materials for fabricating composite include only 3D orthogonal glass fibre fabric, Elium 188 (thermoplastics resin) and Epoxy Epolam 5015 (thermosetting resin) provided by Arkema. After the composite panels are produced, samples will be prepared by cutting the composite panels at angles of 0 degree, 45 degrees and 90 degrees only. Failure mode of 3D woven composite will then be inspected through direct observation after being subjected to bending load. Besides, numerical approach will be adopted to provide an even more thorough insight on the effect of off-axis angles on the flexural properties of thermosetting and thermoplastic 3D woven composites. Simulation model will be established by inputting data provided by third party using ABAQUS software.

## **CHAPTER 2**

### **LITERATURE REVIEW AND THEORY**

#### **2.1 Resin Matrix**

While fibres play the key role in determining the strength and stiffness of a composite material, the service temperature, viable processing approaches and long-term durability of fibre reinforced composites are decided by the selection of matrix materials. Production of advanced high-performance composites requires polymer matrix which can be divided into two categories, namely thermoplastics and thermosetting.

Thermoset is a relatively low molecular weight semisolid that melts and flows during the initial part of the cure process [6]. During cure, the molecular weight increases and the viscosity increases until gelation point, forming strong covalent bond. Crosslinking network are formed during chemical reactions that are driven by heat generated either by the exothermic heat of reaction or externally supplied heat which is normally applied to reduce the curing time. As a result, high-performance thermoset systems require step to elevate their toughness as they inherit brittleness from the high crosslink densities. Moreover, thermosets cannot be reprocessed and will thermally degrade and eventually char if being subjected to sufficiently high temperature due to their highly crosslinked structures. Another potential disadvantage of thermosets is their high moisture absorption. Cured thermoset parts absorb moisture from the atmosphere, which cripples their elevated temperature performance.

Unlike thermosetting polymers, thermoplastics are high molecular weight resins that are fully reacted prior to processing [6]. During processing, they melt and flow during processing but do not form crosslinking reactions as their main chains are held together by relatively weak secondary bonds instead. Nonetheless, the high molecular weight has caused the viscosities of thermoplastics to be orders of magnitude higher than those of thermoset. This has contributed to longer time needed for infusion of composite panel with thermosetting resin. Looking at the good side of



thermoplastics, they can be reprocessed as they do not crosslink during processing. For instance, they can be thermoformed into structural shape by simply reheating to the processing temperature. However, multiple processing will eventually degrade the resin as the processing temperatures are close to polymer degradation temperatures and therefore the number of times a thermoplastic can be reprocessed is limited. On the other hand, thermoplastics absorb very little moisture and thus the design does not have to take such a severe structural knockdown. Figure 2.1 shows the comparison of thermoset and thermoplastic polymer structures [6].

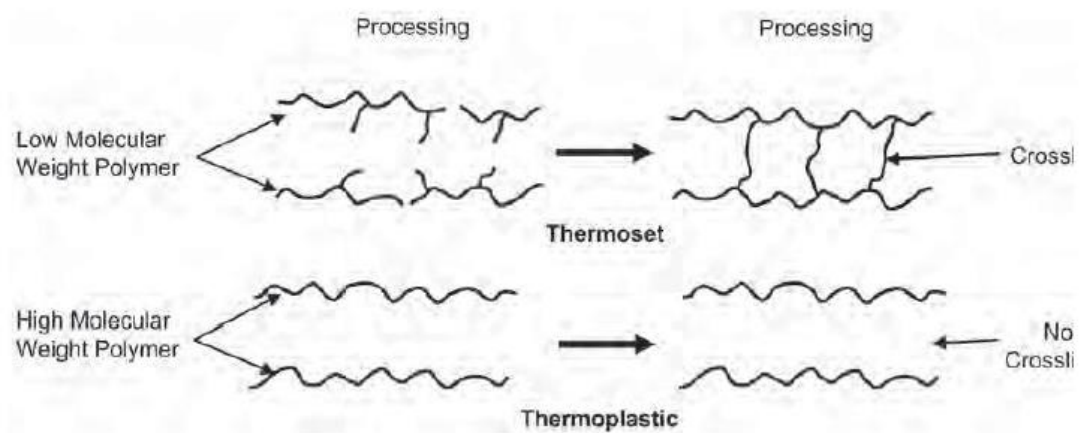


Figure 2.1: Comparison of thermoset and thermoplastic polymer structures [6]

## 2.2 Flexural Properties of 3D Composites

After decades of research and development, 2D composite have reached its limit in terms of flexural modulus and flexural strength. Better understanding on how different parameters could affect the flexural properties of 3D composite is required to overcome the bottleneck of research in composite manufacturing. To date, the parameters being tested includes but not limited to fabric structures, direction of cutting composite samples, resin toughness, classes of 3D weaves, type of composites and fibre contents.

In terms of fabric structures, 3D braid and 3D woven composites behave differently due to their distinct reinforcing preform architectures [7]. The result shows that orthogonal yarn arrangement has provided greater flexural properties for 3D woven composite whereas 3D braid composite has relatively low flexural properties. In the same experiment, 3D braid (BR), 3D woven composites (WV) and 3D woven

composites with twisted yarns (TY) are tested along waft and weft direction. Significance difference is exhibited by 3D woven composite in flexural properties between the two tests direction. The flexural properties in transverse axis are drastically higher than those in the longitudinal axis by around 31% for strength and 46% for modulus. Similar result is also observed when the flexural strengths of 3D braid composite in both directions vary significantly with the longitudinal directions showing higher flexural strength due to its strong anisotropic behaviour. However, there is less direction dependence in flexure in 3D woven composite with twisted yarns, with less than 10% difference in flexural properties in warp and weft direction, showing that flexural properties are more structure dependent. Flexural test curves for these three composites are shown in Figure 2.2.

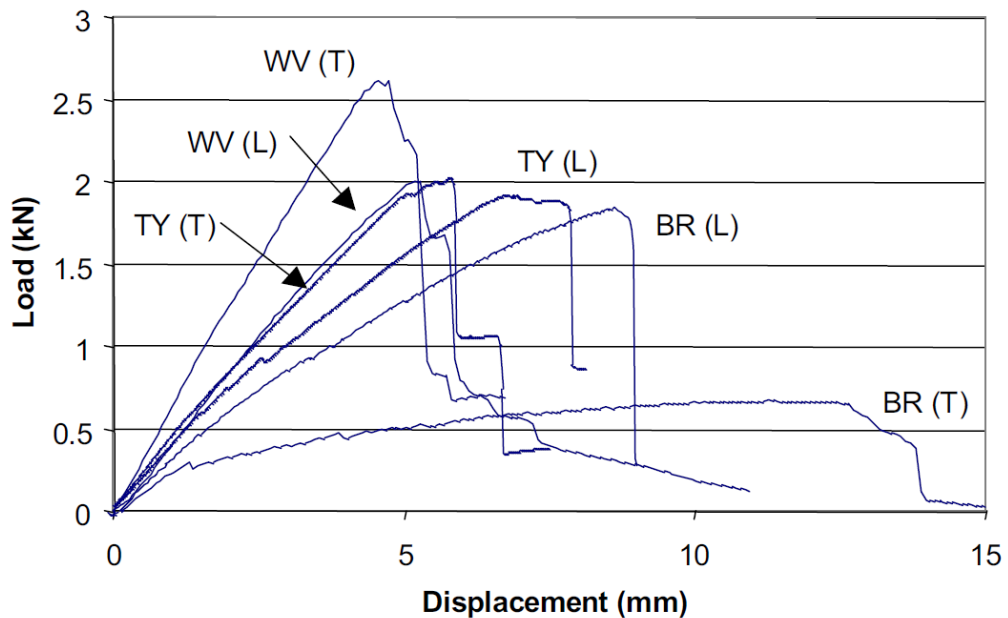


Figure 2.2: Typical flexural test curves [7]

In terms of direction of cutting composite samples, the superiority of the flexural properties of 3D composite in weft direction mentioned earlier is agreed and proven in an experiment conducted to test the flexural properties of 3D orthogonal, angle interlock and layer-to-layer woven composites in warp and weft directions [8]. Among the three composites, large difference is observed in flexural properties in warp and weft directions of the layer-to-layer composite whereas the orthogonal and angle interlock woven composite only show minor difference in flexural properties in both directions. Nonetheless, it is still verified that sample cut along the weft direction

offers higher flexural strength as compared to its counterpart along warp direction. Similarly, the measured value of flexural strength of composite sheets made of 14 and 18 fibre-layers which is 287 MPa, is significantly higher than that in warp direction which is only 218 MPa [9]. Taking a step away from conventional approach that tests only on-axis behaviour, off-axis angles are studied to evaluate its impact on flexural properties. With this purpose, flexural properties of 3D angle interlock woven composite with different angles at 0 degree, 30 degrees, 45 degrees and 90 degrees are tested [10]. It is found that the nominal maximum stresses for four kind of samples with different angles at 0 degree, 30 degrees, 45 degrees and 90 degrees are 960.41 MPa, 480.61 MPa, 422.71 MPa and 1020.21 MPa. Besides, the nominal initial modulus of 90 degrees sample (84.15 GPa) exceeded that of 0 degree sample (81.6 GPa) by 3.13%, that of 30 degrees sample (39.96 GPa) by 110.19% and that of 45 degrees sample (22.77 GPa) by 214.44%. As for the ranking for the strain to the maximum stress, the test sample with 45 degrees was ranked first, followed by 30 degrees, 90 degrees and 0 degree. This concludes that 30 degrees and 45 degrees samples show lower flexural strength, initial modulus and larger flexural deflection as compared to 0 degree and 90 degrees samples.

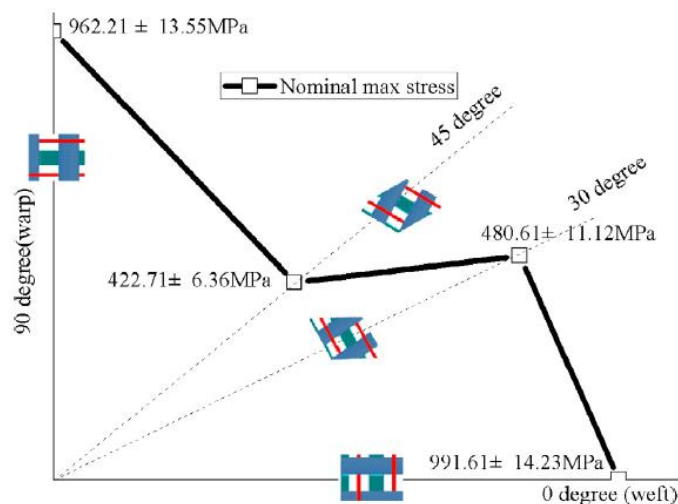


Figure 2.3: Maximum stress of four kinds of angle samples [10]

In terms of resin toughness, 3D angle interlocked woven composites infused with thermoset resin and thermoplastics resin are subjected to three point bending test to investigate their flexural properties [11]. As for the result, 3D thermoset woven composite outperforms 3D thermoplastics in terms of flexural strength, flexural

modulus and its strain to failure rate. The flexural strength, flexural modulus and strain to failure rate are 816.4 MPa, 51.0 GPa and 1.9% for 3D thermoset woven composite as compared to 559.6 MPa, 49.0 GPa and 1.5% for 3D thermoplastics woven composite.

In terms of classes of 3D weaves, 3D orthogonal, 3D warp interlock and 3D angle interlock woven composites are studied to compare their flexural properties [12]. The results reveal that 3D orthogonal woven composite has the lowest stress which is followed by warp interlock and angle interlock based composites. Taking a closer look into 3D orthogonal woven composite, the flexural strength of 3D orthogonal layer-to-layer interlock fabric structures, including warp, weft and bi-directional interlocks along warp and weft direction is investigated [13]. It is found that bi-directional interlock sample has higher maximum force bearing values in both the warp and weft directions in comparison to warp and weft interlocks due to its stacking sequence. Moreover, bi-directional interlock sample elongates less due to the presence of interlocking yarns in both the directions. More importantly, flexural strength and flexural modulus of bi-directional interlock sample are better than the warp and weft interlock samples due to the presence of higher number of interlocking points, making it a more compact structure.

In terms of type of composites, the results from several experiments agree with each other that the flexural properties of 3D composite are superior than that of 2D composite. For instance, it is observed that plain 2D and unidirectional fabric reinforced composites possess higher flexural strength than any 3D counterpart in warp direction for comparable fibre volume fraction [12]. On the other hand, the normalized flexural strength of 3D-weft and 3D-warp samples are both 42% higher than that of the 2D sample while the normalized flexural moduli of 3D-weft and 3D-warp samples are 32% and 28% higher than that of the 2D sample [14]. Similarly, the flexural strength of 3D composites is around 24% more than the plain weave composite when optimum fibre content is considered [15]. There are two reasons as of why the normalized flexural strengths and flexural modulus of 3D composites are higher than 2D composite in both warp direction and weft direction [16]. Firstly, delamination is avoided by having the z-yarn in the thickness direction of the 3D composites. Second, yarns in the fabric interlaced in 2D fabrics slip easily than parallel yarns arranged in the 3D fabrics.

In terms of fibre contents, an experiment is conducted to study the flexural

strength of 3D orthogonal weave composites with different weight fraction of fibres (FWF) of 40%, 45%, 50% and 55% [15]. The result shows that 3D composite has higher flexural strength as the fibre content increases, giving the best result at a fibre weight fraction of 55% as shown in Figure 2.4. This is mainly due to better resin infusion associated with single ply of fabric. Another experiment is carried out to investigate the flexural properties of 3D non-crimp orthogonal composites with different z-binder volume fraction and the geometric data of the reinforcements is shown in Table 2.1 [17]. Due to the highest volume fractions of z-binder, sample 2 with volume fraction of 49.85% has the largest bending strength and modulus. Besides, largest strain of around 5% is exhibited by sample 3 for the epoxy dominated region due to the smallest total fibre volume fraction. Moreover, sample 3 demonstrates the smallest fracture strength although the z-binder packing density is doubled compared to sample 1 and 2. This indicates that the improvement of 3D non-crimp orthogonal composites could not be achieved through increasing packing density. The flexural test curves for these three samples are illustrated in Figure 2.5.

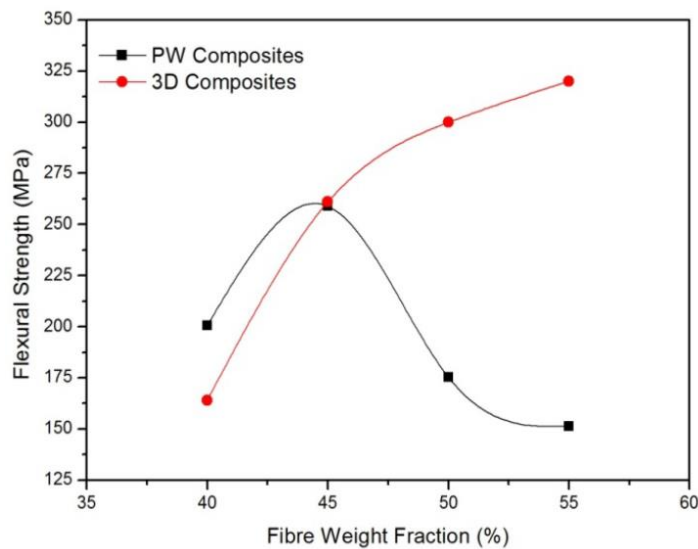


Figure 2.4: Variation in flexural strength [15]

Table 2.1: Geometric data of the reinforcements [17]

Sample	1	2	3
Yarn fineness (K)			
x-axis yarn	12	12	12
y-axis yarn	12	12	12
z-axis yarn	6	12	6
Packing density of z-binders	1	1	2
Thickness (mm)	6.0	6.0	6.0
Areal weight (g/mm <sup>2</sup> )	0.0014	0.0016	0.0012

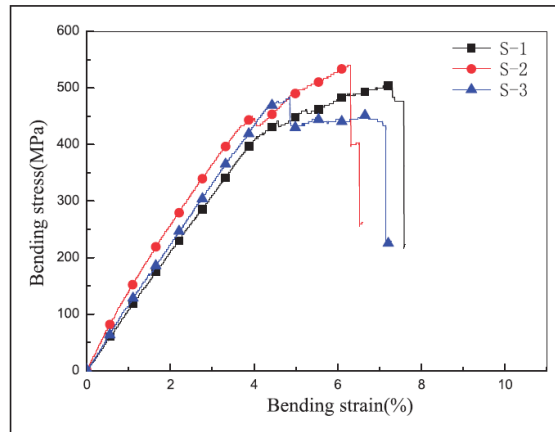


Figure 2.5: Typical morphologies of bending failure for different z-binder volume fraction [17]

### 2.3 Damage Modes of 3D Composites

There are several inspection techniques employed to observe the damage mode of 3D composite, including X-ray microtomography (XCT), visual inspection, immersion focused ultrasound scanning images, acoustic emission technology (AET), optical microscopy, scanning electron microscope (SEM) and so on [8,10,11,14,15,17,18]. Through numerous literature reviews, it is interesting to note that parameters that affect the flexural properties of 3D composites might not have impact on the damage mode suffered by the 3D composite.

Regardless of classes of 3D weaves, 3D orthogonal, angle interlock and layer-to-layer woven composites would experience the same crack propagation initiated from resin-rich areas around z-binder yarns after being subjected to three-point bending load [8]. The crack continues to grow until delamination occurs in warp layer as shown in figure 2.6. Similarly, 3D orthogonal, warp interlock and angle interlock

woven composites will have the crack initiated on the tension side of the beam and slowly propagate in an upward direction [12]. Should a composite fail in tension, it can be due to brittle failure, fibre pull-out, kinking, microbuckling, shear or splitting.

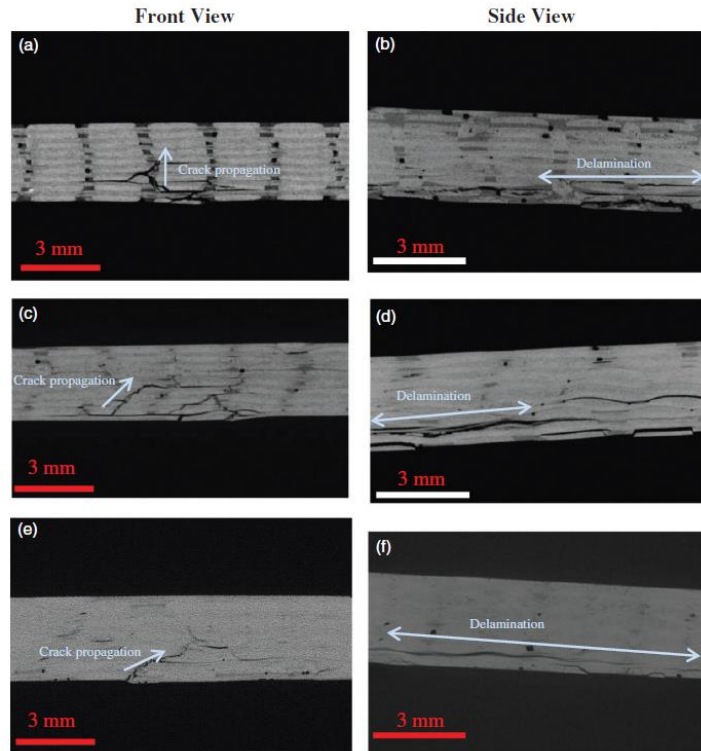


Figure 2.6: XCT scans of front and side of samples tested after flexural tests (a, b) orthogonal, (c, d) angle interlock, and (e, f) layer to layer [8]

Besides, changing the fibre contents does not have impact on the damage mode of 3D composite [15]. Even though different fibre contents of 40%, 45%, 50% and 55% are tested, the result shows that failure in 3D composite for all fibre content is a combination of tensile failure and delamination with opaque zone around the loading region being an indication of delamination. However, an experiment conducted on 3D non-crimp orthogonal composites with different z-binder volume fraction present results which disagree with the previous finding and the geometric data of the reinforcements in presented in Table 2.1 [17]. The results disclose that sample 1 suffers z-binder breakage along with slight pull-out while severe detach of z-binder from the original vertical plane is exhibited by sample 2. As for sample 3, increased packing density has led to development of micro cracks around the fracture surface as the surface yarns are pushed sideways to make space for z-binder, forming a gap between adjacent yarns which then causes local polymer-rich regions on the surface. Moreover,

changing the type of composites from 2D to 3D does have impact on the damage mode where 3D composite suffers less delamination as it has smaller opaque zones than the plain weave composite [15]. Figure 2.7 shows the typical failure modes for the 3-point bending test of 3D and 2D composites [14]. Both composites fail in such a way that they would break at mid span where the central pin is located with the top surface suffering compression load and bottom surface suffering tensile load during the bending test, resulting in highly similar fracture appearances.

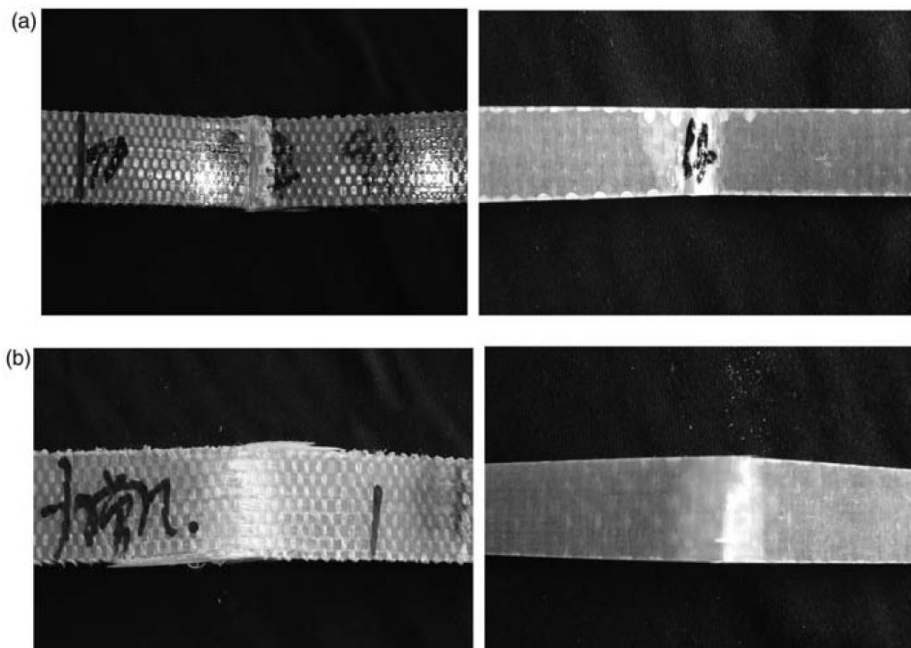


Figure 2.7: Failure mode after 3-point bending test (left: 3D composite; right: 2D composite). (a) front surface; (b) rear surface [14]

Interestingly, the direction of cutting sample has effect only on the damage mode between 3D composite sample cut along on-axis and that cut along off-axis [10]. For example, the damage mode of 3D orthogonal woven composites cut at 0 degree and 90 degrees consist chiefly of matrix cracking, debonding at fibre and matrix interface, and fibre breakage after being subjected to three-point bending load [18]. The cracks of the upper and lower surfaces extend along the warp and weft direction while the cracks propagate from the surface to the interior. The damage process is divided into five stages which are damage initiation, damage growth, destructive damage initiation, destructive damage growth and ultimate failure. Similarly, another experiment has shown that 0 degree and 90 degrees samples suffer similar damage



modes such as kinking, matrix crack, tows debonding, intra-ply delamination and fibre bundle fracture [10]. However, for 30 degrees and 45 degrees samples, the observed damage modes are mostly the same as that for on-axis samples except that no delamination occurs as shown in Figure 2.8.

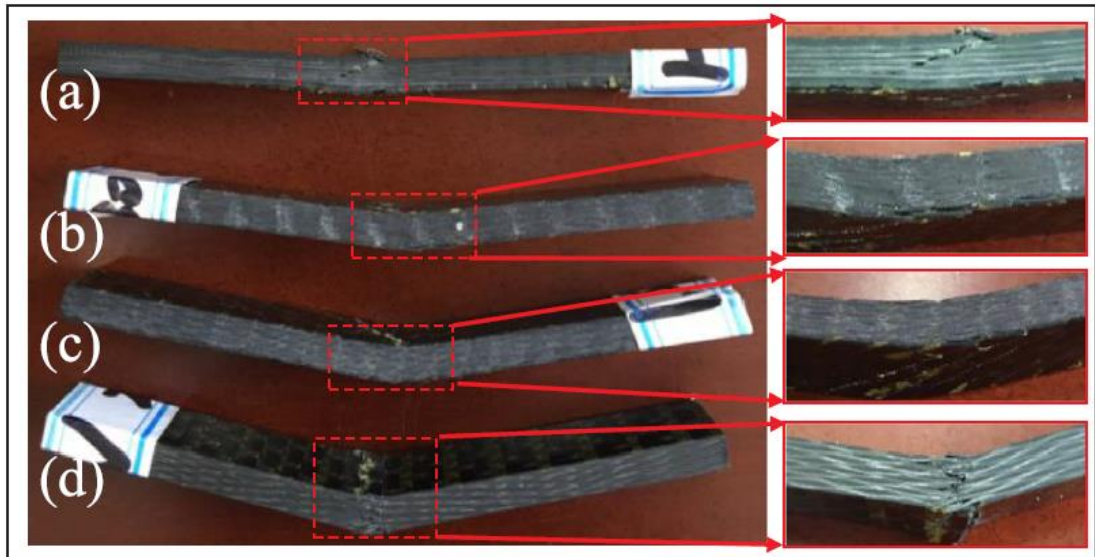


Figure 2.8: Macro failure modes of 0 degree sample (a), 30 degrees sample (b), 45 degrees sample (c) and 90 degrees sample (d) [10]

From the above review of the previous study, it has been discovered that most of the researches focused mainly on investigating the flexural properties of 3D composite reinforced by thermoset but results with thermoplastics resin were scarce. On the other hand, there is totally no research that has explored the difference between thermosetting and thermoplastic 3D composite in terms of flexural properties. More understanding on the mechanical behaviour of thermoplastic based composite is highly desirable as thermoplastic is beneficial towards sustainable development of composite manufacturing industry owing to its recyclability. As with any researches, it is a common practice to describe the failure mechanism of 3D composite subjected to bending load.

# CHAPTER 3

## METHODOLOGY

### 3.1 Project Activities

The project starts with identification of problem statement and objectives and is continued with intensive reading of past research and journal papers to produce critical analysis of literature review. Having established clear understanding on the topic being studied, the project is then continued with preparation of samples through vacuum infusion process. Prior to cutting the samples into desired dimension, the newly infused composite panels have rough surface that needs to be filed using sand paper. Next, the samples are loaded one by one onto universal testing machine according to standard configuration for three-point bending test and are tested till the point of failure. Due to the financial and time constraint, the bending behaviour of 3D woven composite are to be explored thoroughly through simulation of three-point bending test in ABAQUS, rendering it possible to discover to what extent composites which are cut at different angles will fail within a short time frame. The project workflow is illustrated below:

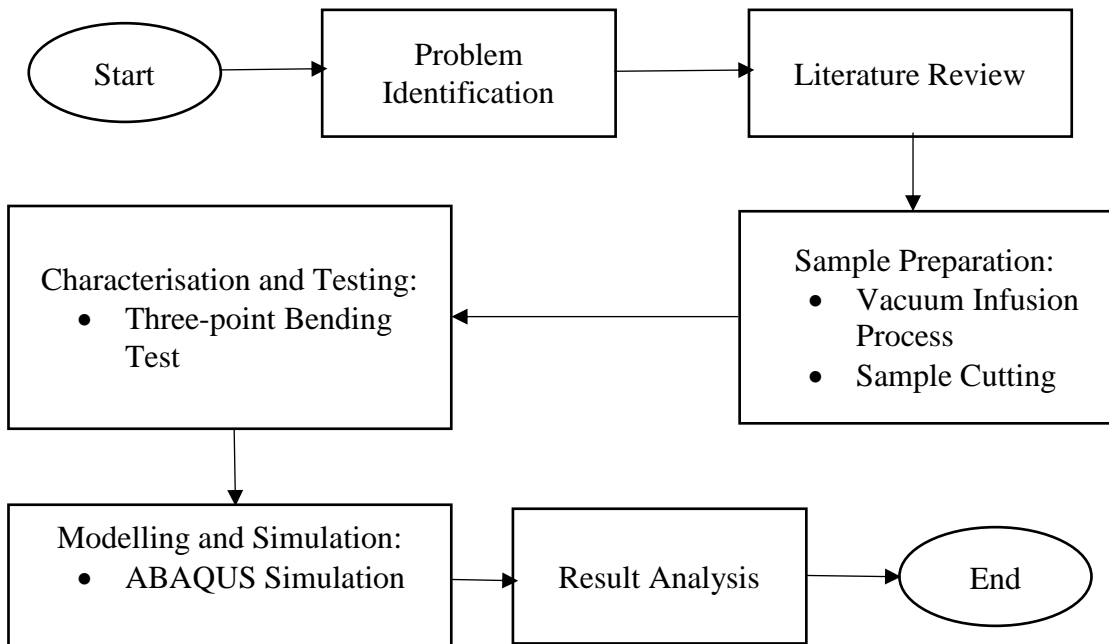


Figure 3.1: Project Workflow

### 3.2 Vacuum Infusion Process

The materials used for fabrication of composite panels are 3D orthogonal glass fabric, Elium 188 (thermoplastics resin) and Epoxy epolam 5015/5015 (thermosetting resin) and a glass mould. Resin is mixed with hardener in the ratio of 7 to 3 by their mass. Figure 3.2 shows a typical setup for vacuum infusion process with arrows showing the direction of resin flow across the composite panel and excess resin will be collected at the resin trap. Before resin starts to infuse the panel, it is important to check for leakages in the vacuum bag by taking reading from the pressure gauge fitted on the resin trap. There is one step to be taken note during fabrication of the composite panel, which is adjustment of pressure for resin infusion. For infusing thermosetting composite panel, the pressure is set at roughly 0.8 bar, allowing higher flow rate of resin across the panel. However, the pressure is reduced to 0.1 bar for the infusion of thermoplastics composite panel to reduce void content which is caused by the vaporization of the highly volatile thermoplastics resin. After the completion of resin infusion, the composite panel is left to be cured under room temperature for 24 hours, followed by post curing at 120 degree Celsius for 3 hours in an oven.

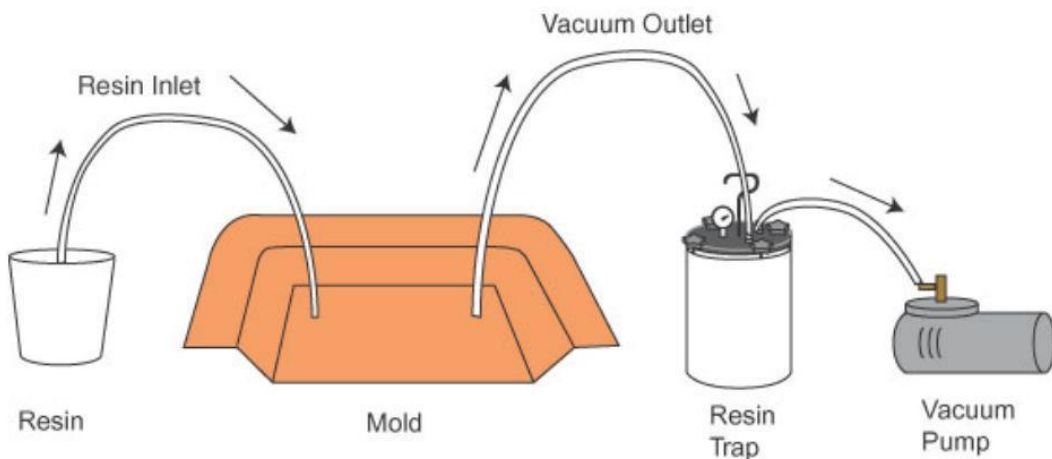


Figure 3.2: Setup for vacuum infusion process

### 3.3 Three-point Bending Test

Prior to conducting three-point bending test, the sample needs to be prepared by first filling the surface of the composite panel to obtain smooth surface. With the aid of protractor, angles of 0 degree, 45 degrees and 90 degrees are measured and marked on the composite panel. Next, the dimension of each sample is set at 150mm x 25mm x

4mm (length x width x thickness) and is marked on the composite panel. A total of 18 samples are then cut out using composite cutting machine and the specification of each sample are tabulated in Table 3.1.

Table 3.1: Specification of samples

Type of resin	Angle of cutting	Number of samples
Thermoplastics	0 degree	3
	45 degrees	3
	90 degrees	3
Thermoset	0 degree	3
	45 degrees	3
	90 degrees	3

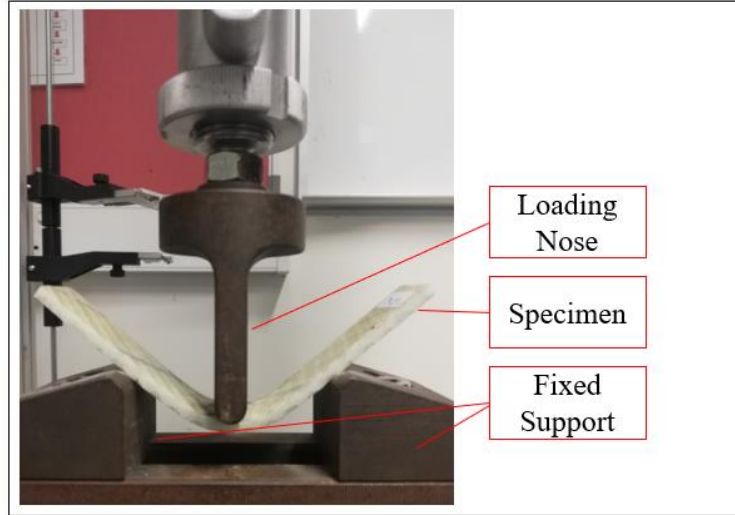


Figure 3.3: Setup of three-point bending test

Next, three-point loading configuration is set up on a universal testing machine according to ASTM D7264 as shown in Figure 3.3. The sample is loaded onto the machine in such a way that the span to thickness ratio is 16:1. Then, the test starts and the crosshead displacement rate is maintained at 2mm/min. During the process, the deflection of the sample is measured and recorded automatically. Then, flexural strength ( $\sigma$  in MPa), flexural strain ( $\varepsilon$  in %) and flexural modulus (E in GPa) and energy absorption (EA in MJ/m<sup>3</sup>) are computed through equations 3.1 to 3.4

$$\sigma = \frac{3PL}{2bh^2} \quad \text{eq. 3.1}$$

$$\varepsilon = \frac{6\delta h}{L^2} \times 100 \quad \text{eq. 3.2}$$

$$E = \frac{y_2 - y_1}{x_2 - x_1} \cdot \frac{L^3}{4bh^3} \quad \text{eq. 3.3}$$

$$EA = \sum_1^{n-1} [0.5(\sigma_{n+1} + \sigma_n)(\varepsilon_{n+1} - \varepsilon_n)] \quad \text{eq. 3.4}$$

where P (N) is the applied force, L (mm) is the support span, b (mm) is the width of the beam, h (mm) is the thickness of the beam  $\delta$  (mm) is the mid-span deflection,  $y_1$  and  $y_2$  (MPa) are any two values of flexural strength along the linear region of the stress-strain curve,  $x_1$  and  $x_2$  (%) are the corresponding values of flexural strain along the linear region of the stress-strain curve and n is the number of data points taken. On a side note, energy absorption is calculated using the trapezoidal rule which is a technique for estimating the definite integral.

### 3.4 Finite Element Analysis

As there is a limit to the amounts of samples that could be tested using experimental approach, finite element analysis will be employed to execute a more holistic study on the effect of off-axis angle on the flexural strength of both thermosetting and thermoplastic 3D woven composite. This is done by establishing a simulation model subjected to three-point bending load at macro-scale level in ABAQUS simulation software. To begin with, a rectangular structure which represents the specimen will be constructed with dimension of 100mm x 25mm x 4mm (length x width x thickness). Next, a half cylinder which represents the loading nose and supports is created by first drawing a half circle with radius of 3mm and then extruding it by 25mm. The rectangular structure is then assembled with the half cylinders according to ASTM D7264 where the loading nose is placed at the middle while the supports are placed at 32mm away from the middle. The configuration of the simulation model is shown in Figure 3.4.

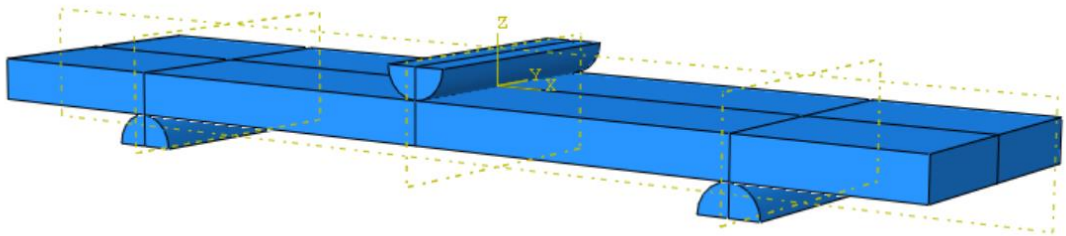


Figure 3.4: Setup of three-point bending load in simulation

Next, the material properties for both structures need to be defined. For composite, its elastic mechanical behaviour will be described by nine mechanical

properties which are Young's modulus, shear modulus and Poisson's ratio along three axes and planes as listed in Table 3.2. To simulate damage initiation, hashin damage criterion is chosen and will be described by another six mechanical properties which include tensile strength, compressive strength, and shear strength in longitudinal and transverse direction as listed in Table 3.3. As for supports and loading nose, they will be assumed as steel which are defined by just Young's modulus and Poisson's ratio as shown in Table 3.4.

Table 3.2: Elastic mechanical behaviour of composites

Resin	E <sub>1</sub> (GPa)	E <sub>2</sub> (GPa)	E <sub>3</sub> (GPa)	v <sub>12</sub>	v <sub>13</sub>	v <sub>23</sub>	G <sub>12</sub> (GPa)	G <sub>13</sub> (GPa)	G <sub>23</sub> (GPa)
TS	26.3	26.0	12.5	0.11	0.11	0.11	4.5	4.0	4.0
TP	15.0	15.0	6.0	0.12	0.12	0.12	4	2.5	2.5

Table 3.3: Material properties of composites for hashin damage criterion

Resin	T <sub>L</sub> (MPa)	C <sub>L</sub> (MPa)	T <sub>T</sub> (MPa)	C <sub>T</sub> (MPa)	S <sub>L</sub> (MPa)	S <sub>T</sub> (MPa)
TS	257	450	300	414	45	45
TP	293	478	357	458	40	40

Table 3.4: Elastic mechanical behaviour of supports and loading nose

Material	Young's modulus (GPa)	Poisson's ratio
Steel	210	0.35

Next, two sections will be created as homogeneous continuum shell element for beam and homogeneous solid element for half cylinders before assigning to them. Before defining material orientation, a local coordinate system needs to be constructed at the centre of the beam as shown in Figure 3.4. The material orientation is first fixed at 0 degree relative to the coordinate system and there will be an increment of 15 degree for each succeeding simulation. Then, the global seed sizes are set at 0.0032 for the beam structure and 1 for the half cylinders. On top of that, local seed size is set at 0.0005 for the cross section of beam structure before applying mesh to them to increase the accuracy of results. The simulation model with mesh is shown in Figure 3.5.

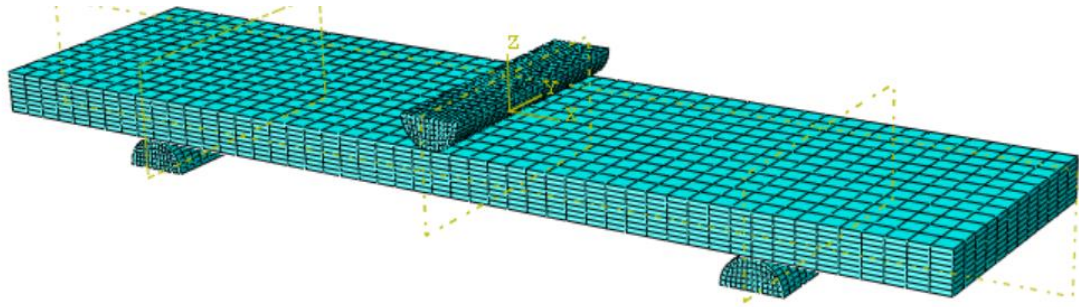


Figure 3.5: Simulation model with mesh

To define the surface that will deform, interactions between the supports, loading nose and the surfaces of the beam need to be defined where the deformable beam is selected as slave surface while the rigid supports and loading nose are selected as master surfaces. Example of defining interaction is shown in Figure 3.6 that indicates master surface and slave surface as red region and pink region respectively. In order to ensure the beam could deform in z direction without moving sideways, four boundary conditions need to be defined at four different locations with respect to the local coordinate system as listed in Table 3.5. All values for boundary conditions are fixed except for the z-displacement applied by the loading nose because this value is input in a trial and error manner until the hashin damage criteria is closed to or reach 1.

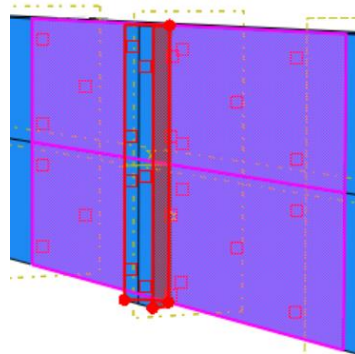


Figure 3.6 Interaction between loading nose and beam

Table 3.5: Boundary conditions on the simulation model

Location	Translation along x direction (mm)	Translation along y direction (mm)	Translation along z direction (mm)	Rotation about x-axis (radian)	Rotation about y-axis (radian)	Rotation about z-axis (radian)
Loading nose	0	0	dependent	-	-	-
xz plane of beam	-	0	-	-	-	-
yz plane of beam	0	-	-	-	-	-
Supports	0	0	0	0	0	0

Next, automatic step is created with initial increment size of 0.01, minimum size of 0.00001, maximum size of 1 and maximum number of increments of 1000. Lastly, the default field output request needs to be edited by adding damage initiation criteria and VUMAT before creating job to run the simulation.



### 3.5 Gantt Chart

The project timeline is shown in the Gantt chart in Table 3.6.

Table 3.6: Gantt chart

Progress	Week Number	FYP I														FYP II													
		1	2	3	4	5	6	7	8	9	10	11	12	13	14	1	2	3	4	5	6	7	8	9	10	11	12	13	14
Topic Selection		█																											
Literature Review			█	█	█	█	█	█																					
Vacuum Infusion Process						█	█	█	○																				
Sample Cutting									○	○																			
Three-point Bending Test											█	█	█	○															
ABAQUS Simulation																█	█	█	█	█	█	█	█	█	█	○			
Documentation																							█	█	█				
Project Presentation																									█	█	█		

### 3.6 Project Key Milestones

Project key milestone for FYP I and FYP II are presented in Table 3.7 and 3.8 respectively.

Table 3.7: Project Milestone of FYP I



<b>Project Milestone</b> 	
<b>Week</b>	<b>Activities</b>
9	Completion of Vacuum Infusion Process
10	Completion of Sample Cutting
14	Completion of Three-point Bending Test

Table 3.8: Project Milestone of FYP II

<b>Project Milestone</b> 	
<b>Week</b>	<b>Activities</b>
12	Completion of ABAQUS Simulation

## CHAPTER 4

### RESULTS AND DISCUSSIONS

#### 4.1 Three-point Bending Test

Figure 4.1 depicts flexural stress strain curves of six kinds of samples with varied resins and angles which are tested at a span-to-thickness ratio of 16:1. Every curve is a representative sample for each orientation, which provides a complete depiction of changes in the specimen stiffness as well as the damage initiation and growth. By viewing the samples made of the same resin at a time, the bending mechanical behaviours are indicated as being sensitive to the off-axial orientation when the stress strain curves virtually show distinctive trends for three varieties of angles of specimens.

Besides, comparing the curves at each orientation reveals the fact that thermoplastic samples demonstrate slightly greater ductility than their thermosetting counterparts as the stress strain curves for thermoplastics samples are invariably placed below that for thermosetting samples at any orientation. This is because the molecular chains of thermoplastics samples are not held together by crosslinking structures, enabling the molecules to slide past each other under high stress and thus able to deform further instead of experiencing abrupt breakage. This also shows that the type of resin only has minor effect on the bending mechanical behaviours of composite structures. Moreover, it is discovered that the damage processes and failure modes vary significantly with the change of off-axis angle and this phenomenon will be verified further in next section with SEM diagrams for the tested samples.

For 0 degree (weft) and 90 degree (warp) on-axis specimens, the stress strain curves are linear over their full range of strain, eventually terminating in fracture without appreciable plastic flow and this suggested an important brittle behaviour [19,20]. The reason is that the transverse properties of glass fibre bundles are being tested in this case and are inferior in resisting the loads applied on the on-axis samples. On top of that, a sudden drop of stress is observed at 90% of the ultimate strength in the 90 degree sample which is probably due to critical structural damage. On the contrary, little fluctuation is presented in 0 degree sample before experiencing ultimate

fracture. For 45 degree off-axis samples, the stress strain curves are observed to be non-linear and have exhibited large bending deflection with a lower maximum load. This suggests that 45 degree samples have undergone ductile deformation. More importantly, no disastrous damages have occurred suddenly since the stress strain curves of 45 degree samples are smooth.

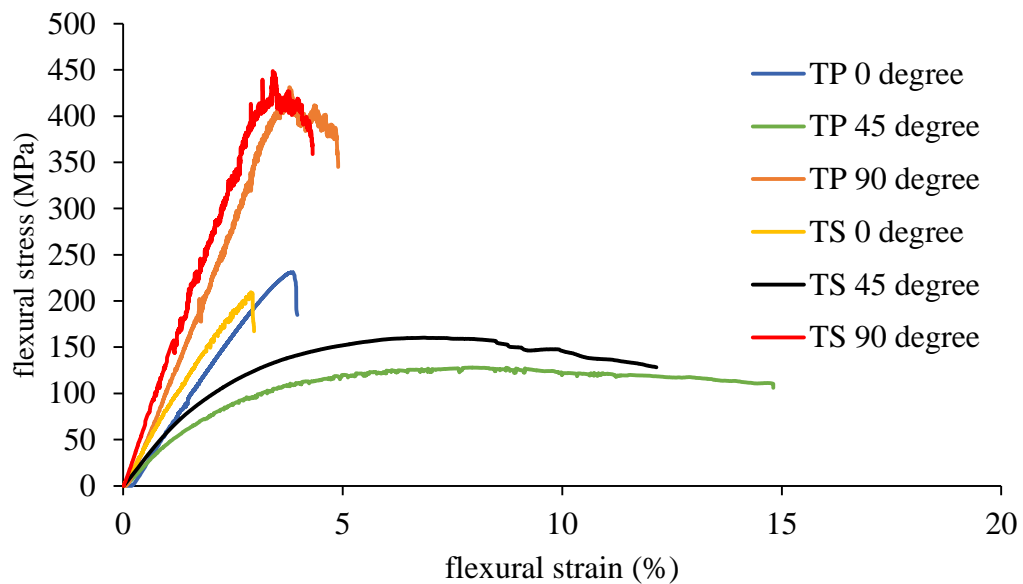


Figure 4.1: Experimental flexural stress strain curve of thermosetting and thermoplastic samples

Determined to present good and precise interpretation of experimental results, Figure 4.2 to 4.5 are used to summarize the key bending parameters which include flexural strength, flexural modulus, flexural strain and energy absorption up to failure for six kinds of samples. As a rule of thumbs, each bending parameter is studied and investigated based on three repetitive experiments and each value will be presented as the average of three samples tested with the standard deviation.

Apparently, it can be inferred that both thermoplastic and thermosetting 3D woven composite display anisotropic characteristics based on all the observed results. From Figure 4.2, it is shown that for three kinds of thermoplastic samples with different off-axis angles, 0 degree, 45 degree and 90 degree, the flexural strength are 249.17 MPa, 135.41 MPa and 418.15 MPa respectively. Similar trend is observed for three kinds of thermosetting samples with different off-axis angles, 0 degree, 45 degree and 90 degree, where the flexural strength are 249.45 MPa, 162.40 MPa and 454.86 MPa respectively.

It can be concluded that 90 degree samples have flexural strength of nearly two times higher as compared to 0 degree samples for both thermoplastic and thermosetting samples. This is because z yarns which are aligned in axial direction in 90 degree samples are perpendicular to the indenter and try to straighten under the bending load, leading to higher flexural strength. In contrast, the flexural strength of off-axis 45 degree samples are so much lower than those of on-axis samples. This could be explained by giving a brief description on the load bearing mechanism of off axis samples.

In an off-axis sample, weft and warp are biased with certain angle. As a result, off-axis sample would try to reorient towards the principal loading axis when subjected to shear loading. Thus, large geometrical deformation will first occur in off-axis sample for the yarns to be adjusted in a way that favours the supporting of bending load. The phenomenon that takes place between warp and weft during the reorientation process is commonly known as “scissoring effect” [21]. This will cause interfacial debonding between the yarns and matrix that results in lower flexural strength.

Moreover, thermosetting samples are shown to possess slightly higher flexural strength as compared to its thermoplastic counterparts. This is mainly due to the increased molecular weight as cross-linking forms in thermoset and the strength of a polymer is in fact proportional to its molecular weight up to a certain limit.

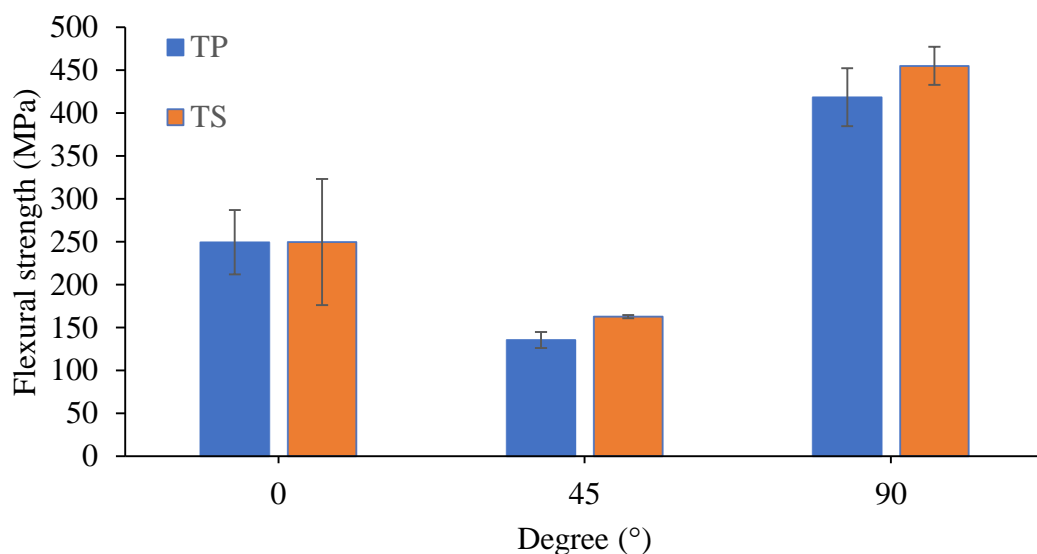


Figure 4.2: Experimental flexural strength of thermosetting and thermoplastic samples

In Figure 4.3, the trends of flexural modulus are shown to be consistent with those of flexural strength. For thermoplastic samples, the flexural modulus of 90 degree sample (12.12 GPa) exceeds that of 0 degree sample (7.62 GPa) by 59.06% and that of 45 degree sample (5.45 GPa) by 122.39%. Observing thermosetting samples, 90 degree sample is ranked first in terms of flexural modulus (14.28 GPa), followed by 0 degree sample (8.91 GPa) and 45 degree sample (6.35 GPa), which are lower by 60.27% and 124.88% respectively.

Generally, the surface rigidity near the loading head has direct correlation to flexural modulus. For off-axis sample, lower flexural modulus stems from the three main load-carrying tows not being fully utilized when they are forced to undergo reorientation. However, higher flexural modulus is demonstrated by on-axis samples due to the ability of the upper surfaces of on-axis samples to maintain the straight weft and warp alignment within the composite structure.

Similarly, thermosetting samples are superior in terms of flexural modulus just as they are in terms of flexural strength. At 0 degree, 45 degree and 90 degree, thermosetting samples have flexural modulus of 16.93%, 16.51% and 17.82% higher as compared to thermoplastic samples. This suggests that changing the resin from thermoplastic to thermoset could raise flexural modulus by almost the same degree regardless of the orientation.

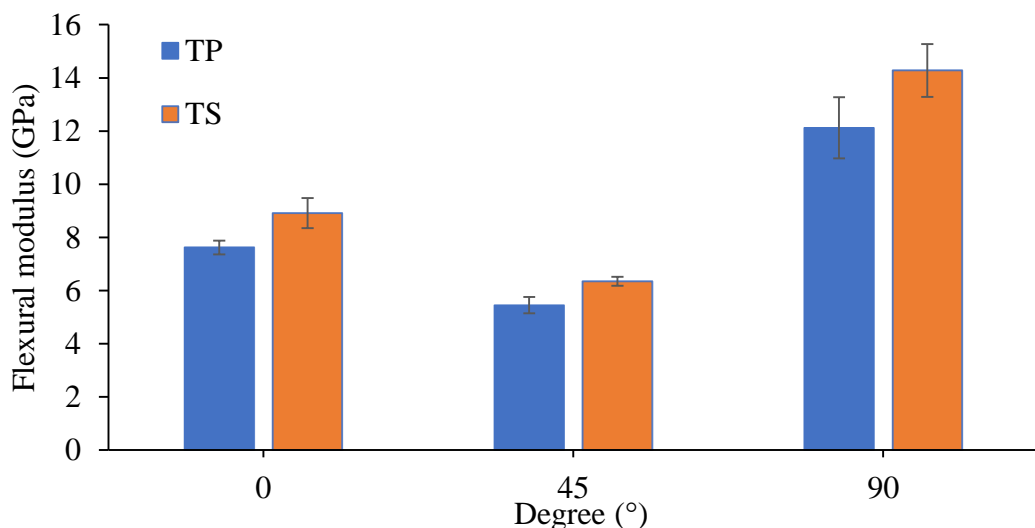


Figure 4.3: Experimental flexural modulus of thermosetting and thermoplastic samples

As shown in Figure 4.4, ranking for the flexural strain is almost contrary to the sequence of flexural strength and flexural modulus. For thermoplastic samples, 45 degree sample has the highest strain (13.42%), followed by 90 degree sample (5.07%) and 0 degree sample (4.32%). For thermosetting samples, the ranking for flexural strains remains unchanged but the flexural strain is relatively lower at each off-axis angle as compared to thermoplastic samples. Similar findings are reported in Ref. [10].

Highest flexural strains are demonstrated by 45 degree samples as their bending mechanical behaviours follow that of a ductile material which experience large geometrical deformation. Besides, thermoplastic samples have higher flexural strains as compared to thermosetting samples because the molecular chains of thermoplastic are not held by crosslinking and therefore have high mobility, enabling relative motion between molecular chains when subjected to loading.

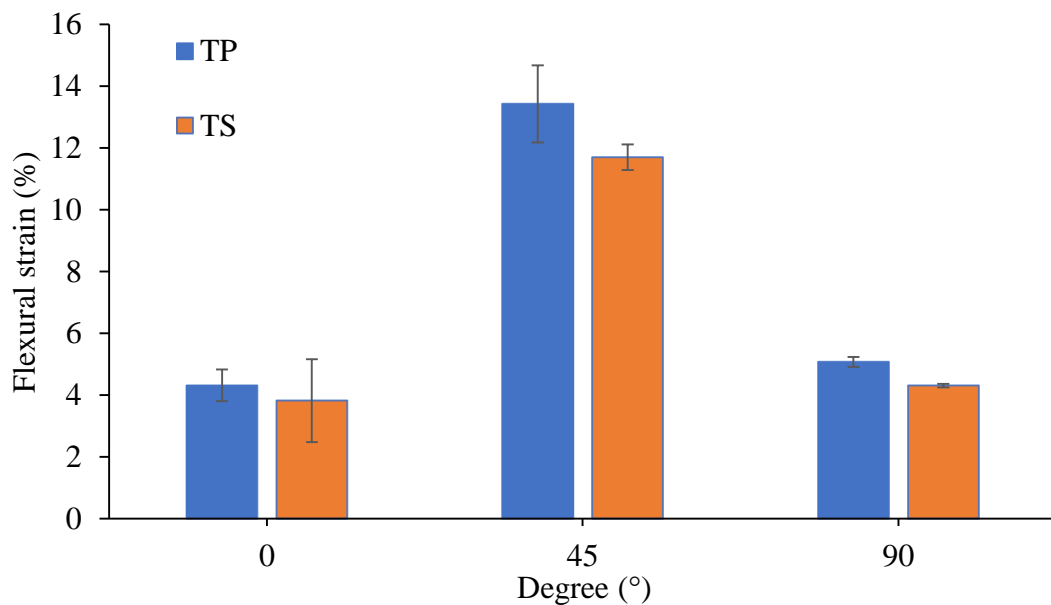


Figure 4.4: Experimental flexural strain of thermosetting and thermoplastic samples

Figure 4.5 illustrates the energy absorption per unit volume up to fracture for six kinds of samples, which is calculated as the area under the stress strain curve using trapezoidal rule. Apparently, the energy absorption of both thermoplastic and thermosetting 3D woven composite subjected to the bending load is heavily influenced by the off-axis angle. For thermoplastic sample, the energy absorption reaches its peak at 1503.05 MJ/m<sup>3</sup> at 45 degree, surpassing that of 90 degree (1237.95 MJ/m<sup>3</sup>) and that of 0 degree (582.50 MJ/m<sup>3</sup>) by 21.41% and 158.03% respectively. Thermosetting

samples follow similar trend with 45 degree sample having the highest energy absorption ( $1540.91 \text{ MJ/m}^3$ ), which is followed by 90 degree sample ( $1159.62 \text{ MJ/m}^3$ ) and 0 degree sample ( $540.64 \text{ MJ/m}^3$ ).

Interestingly, there are only minor differences between the energy absorption of thermoplastic and thermosetting 3D woven composite at each off-axis angle where thermoplastic samples could absorb slightly more energy at 90 degree and 0 degree except for 45 degree. This exception could be attributed to experimental error which is indicated by high standard deviation of about  $131.18 \text{ MJ/m}^3$  for thermoplastic 45 degree sample. In general, off-axis samples are observed to manifest higher energy absorption as compared with on-axis samples and this phenomenon is best explained by the scissoring effect mentioned earlier [21]. Moreover, the increase in energy absorption in thermoplastic samples is also consistent with the higher flexural strains being exhibited by thermoplastic samples.

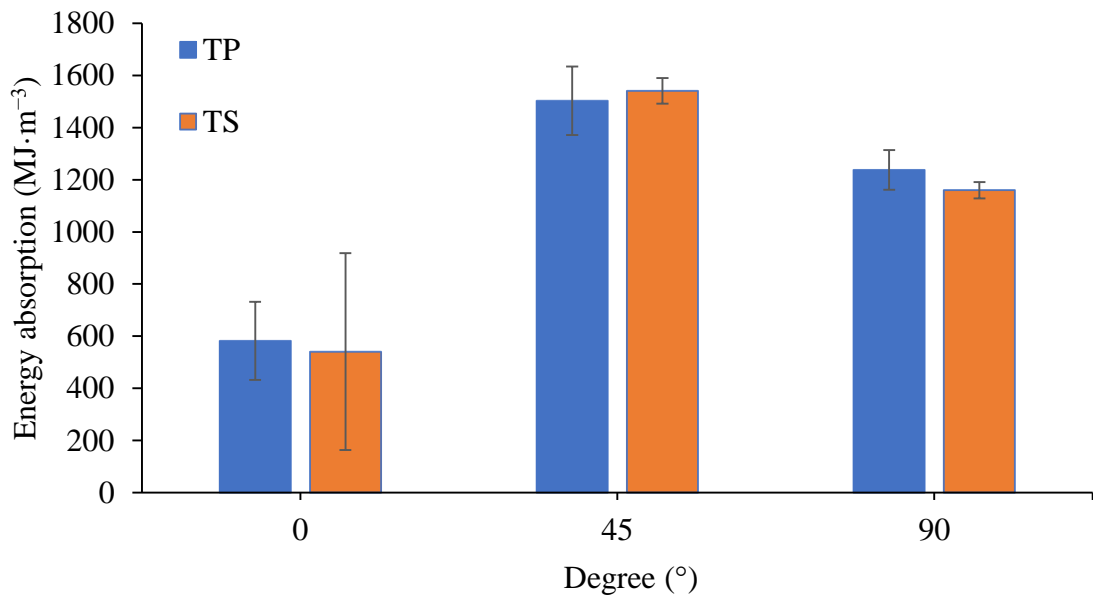


Figure 4.5: Experimental energy absorption of thermosetting and thermoplastic samples

## 4.2 Macro-scale Damage Characterization

Referring to Figure 4.6, it is obvious that each specimen has been inflicted with a certain amount of damage when there are white-coloured regions form right at the mid span of each specimen. The existence of these unique regions allows to postulate that



crevices have been developed underneath the rear surface of the samples. Therefore, it can be inferred that the primary damage mode of all kind of samples is a mixture of tensile failure and delamination. Comparing between 0 degree sample and 90 degree sample, the greater extension of white regions implies that 90 degree sample suffers more delamination than 0 degree sample does. This phenomenon is comparable with higher flexural stress being sustained by 90 degree as compared to 0 degree sample.

Moreover, comparison of thermosetting and thermoplastic samples reveals that thermoplastic samples are more resistive towards delamination as indicated by little or no cracks on their rear surfaces. This is again explained by the fact that thermoplastic samples are acted upon by slightly lower flexural stress as compared to thermosetting samples. In other words, the samples could be arranged in descending order of the amount of delamination within them, starting with thermosetting 90 degree sample, followed by thermosetting 0 degree sample, thermoplastic 90 degree sample and lastly thermoplastic 0 degree sample. Although visual inspection on the rear surfaces of samples could aid in characterization of macro-scale damage, accurate information pertaining to internal damage characteristics such as fibre bundles failure and tow debonding is not obtainable, which hinders comprehensive understanding of failure mechanism of thermosetting and thermoplastic 3D woven composite damaged under bending load.



Figure 4.6: Macro-scale damage on rear surfaces of on-axis samples including thermosetting 0 degree sample (a), thermosetting 90 degree sample (b), thermoplastic 0 degree sample (c), and thermoplastic 90 degree sample (d)

Moving on to macro-scale damage characterization of off-axis samples, similar damage mode is shown in Figure 4.7 where the mid-span of specimen manifest white

region which is an indication of delamination as discussed earlier. Comparison between thermosetting and thermoplastic samples at 45 degree displays consistency in result with that at on-axis angles. It is evident that greater damage has been incurred on thermosetting sample even though that damage is hardly visible and is only observable with close attention. As opposed to that, visual inspection on the rear surface of thermoplastic 45 degree sample could barely spot any damage that it is visually intact as if no load has been applied on it.

Comparing on-axis samples with off-axis samples, superiority of off-axis sample in terms of damage resistance is clearly delineated when the sign of delamination wanes away as angle of cutting sample morphs from on-axis to off-axis. At this stage, it can be deduced that thermoplastic 45 degree sample performs best at resisting delamination. Similar finding is reported in Ref. [10] where there is no apparent delamination found in 45 degree samples unlike 0 degree and 90 degree samples that are fraught with catastrophic and continuous cracks. Those damages are portrayed by the inflection points on the corresponding stress-strain curves.

Although visual inspection on the rear surfaces of samples could aid in characterization of macro-scale damage, accurate information pertaining to internal damage characteristics such as fibre bundles failure and tow debonding is not obtainable. This hinders comprehensive understanding of failure mechanism of thermosetting and thermoplastic 3D woven composite damaged under bending load.



Figure 4.7: Macro-scale damage on rear surfaces of off-axis samples including thermosetting 45 degree sample (a), and thermoplastic 45 degree sample (b)

### 4.3 ABAQUS Simulation

In this section, the global responses of both thermoplastic and thermosetting 3D woven composites under three-point bending load and damage initiation have been predicted at the full-scale beam level. Simulation is performed repeatedly by manipulating the

off-axis angles with an increment of 15 degree each time. This is to investigate the effect of off-axis angle on the flexural strength of 3D woven composites and characteristics of damage as well. All results are obtained at the yield point instead of the fracture point where the simulation halts when hashin damage criterion is closed to or reaches the value of 1. Based on the results from the simulation, a graph is then plotted on the flexural strength of both thermoplastic and thermosetting samples at off-axis angles in the range of 0 degree to 90 degree. It is significant to serve as a visual aid to depict the whole picture of whether thermoplastic sample is superior to its thermosetting counterpart over the whole range of off-axis angles. On the other hand, this section also discusses the possible reasons that render the difference between numerical and experimental results at angles of 0, 45 and 90 degree.

Before explaining the evolution of damage characteristics of 3D woven composites as angles change from 0 degree to 90 degree, it would be necessary to understand what hashin damage criterion implies. Hashin damage criterion is one of the failure criteria that predicts the anisotropic damage in elastic-brittle material and is used primarily for fibre-reinforced materials. Four different failure modes are being considered which include fibre tension, fibre compression, matrix tension and matrix compression. More importantly, damage will initiate within the composites when hashin damage criterion reaches 1 due to either one of failure modes. Taking reference from Figure 4.8(b) to 4.21(b), the damage initiations are only represented in the forms of hashin matrix tension criterion (HSNMTCRT) and hashin fibre fibre tension criterion (HSNMTSRT). The images for hashin matrix compression criterion (HSNMCCRT) and hashin fibre compression criterion (HSNFCCRT) are excluded as the samples only fail due to tension.

To begin with the characterisation of damage, Figure 4.8(b) shows that 0 degree thermosetting yields when fibre cracks at the middle section along transverse direction due to tension. Meanwhile, little damage has been suffered by the matrix as indicated by low value of HSNMTCRT which is roughly about 0.0074. Next, Figure 4.3.9(b) to 4.3.14(b) depict that the damage initiation is solely due to matrix tension at all off-axis angles and 90 degree. This implies that the mechanical strength of resin has become the limiting factor to the maximum stress that can be absorbed by the samples over a wide range of off-axis angles. Therefore, focusing on and increasing the mechanical strength of resin are needed to enhance the flexural strength. However, the area of damage differs with 90 degree thermosetting sample showing largest area

of damage, which is followed by 45 degree, 60 degree, 30 degree, 15 degree and 75 degree thermosetting samples.

Besides, it can be inferred that fibre bears less stress as the angle approaches 90 degree because HSNFTCRT decreases gradually. This phenomenon does make sense because the stress bearing mechanism would shift from fibre-dominant to matrix dominant when the increasing off-axis renders the direction of fibre to be perpendicular to the direction of applied stress. Speaking about the location of damage initiation, it is worth to note that the damage would concentrate at the centre for on-axis samples and at the edge of middle section for off-axis samples. Furthermore, Figure 4.15(b) to 4.3.21(b) provide similar results for thermoplastic sample in terms of location, area and type of damage initiation as compared to thermosetting samples. However, HSNFTCRT is higher in thermosetting samples than in thermoplastic samples for each off-axis angle. This suggests that fibre in thermosetting samples bears more stress which is probably due to better adhesive property between thermosetting resin and glass fibre that allows more even distribution of stress between them. This observation creates the need to research on improving the adhesive property between thermoplastic resin and glass fibre so that glass fibre could share more load with its reinforcement to withstand higher stress in overall.

Moving on to elaborating the stress distribution throughout the specimens as shown in Figure 4.8(a) to 4.21(a), higher stress is observed at the bottom surface of the specimen and hence this stress is taken as the flexural strength. On the contrary, the stress at the top surface is only about half of the stress at the top surface. Since the top and bottom surface experience compression and tension respectively, higher stress at the top surface causes tensile stress to be the key factor that contributes to failure of composite under three-point bending stress as discussed previously when reviewing the hashin damage criteria. Moreover, both thermoplastic and thermosetting samples shows that the stress reaches its peak at the midplane and dissipates along longitudinal direction towards both edges.

Next, Figure 4.22 illustrates the flexural strength of both thermosetting and thermoplastic samples at different off-axis angles. Both thermosetting and thermoplastic samples show similar trend where the flexural strength decreases at decreasing rate at 0 degree until it reaches its minimum at 45 degree before rising at increasing rate until peak is attained at 90 degree. The graph also indicates that thermoplastic samples have higher flexural strength at the range of 0 to 5 degree and

70 to 90 degree. This means that thermoplastic 3D woven composite could replace its thermosetting counterpart in any industrial application that requires high flexural strength given that thermoplastic 3D woven composite is fabricated at off-axis angles at these ranges. However, for industrial application where the total energy absorption at the point of failure is more significant, further study needs to be conducted to find out the range of off-axis angles at which thermoplastic woven composite exhibits high energy absorption. This would require damage evolution to be modelled in finite element simulation instead of solely damage initiation.

Referring to Table 4.1, experimental and numerical results on flexural strength of thermosetting and thermoplastic samples are listed side by side to compute the percentage of error. The main purpose is to verify the accuracy of data generated by finite element analysis. If the numerical results are proven to be accurate, it would bring upon an opportunity to replace experiment with numerical analysis. In this case, not only could the progress of research be accelerated, limitation such as access to equipment and shortage of research fund could be resolved. This is because running a simulation would just require purchasing a computer with good processor and license of simulation software while the progress made by conducting experiment is subject to availability of material and equipment. There is no additional cost incurred to generate numerous results by altering the parameters given that a precise simulation model has been established. If huge disparity exists between numerical and experimental data, critical review of the simulation model is required to improve the accuracy of numerical result to take advantage of the aforementioned benefits.

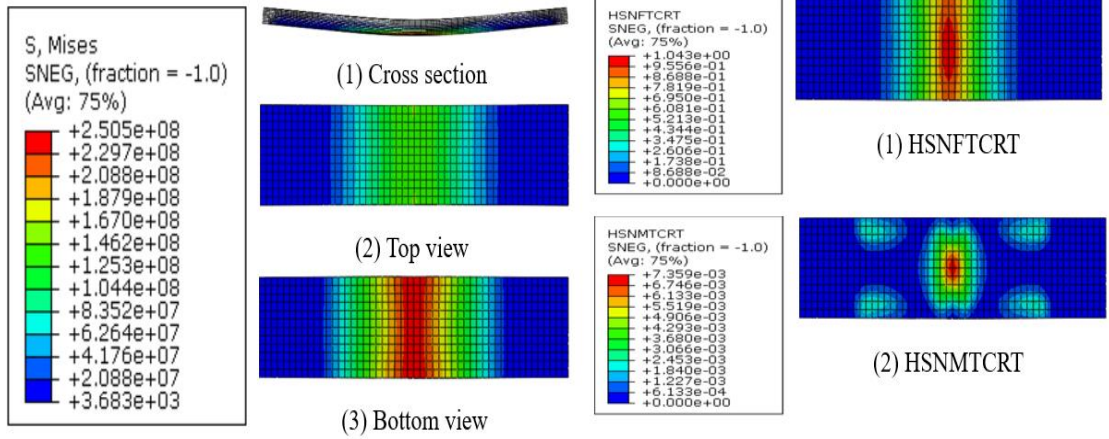
Table 4.1 shows the numerical results being dissimilar to experimental results. According to experiment results, thermoplastic samples have lower flexural strength at angles of 0, 45 and 90 degree. Opposite to that, numerical results suggest higher flexural strength is possessed by thermoplastic sample at on-axis angles except for 45 degree. Computing the percentage of error at each angle reveals the numerical data is slightly inaccurate as the average percentage of error is found to be around 22.97%. Few reasons might have led to this situation.

First, the simulation has disregarded the variation of geometry caused by air pockets formed within the structure of thermoplastic samples. As a recap, thermoplastic resin is highly volatile that it restricts vacuum resin infusion of thermoplastic composite from being carried out at high pressure to prevent forming of massive amount of bubbles. During post-curing process, highly volatile thermoplastic

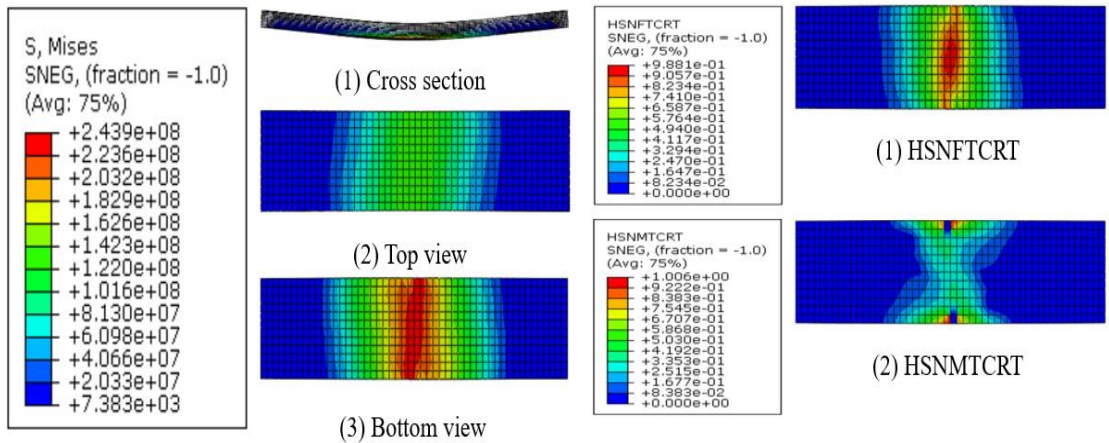
resin would evaporate due to exposure to atmospheric pressure, introducing voids to the structure of thermoplastic samples which jeopardise the structural integrity and thus reduce the flexural strength of that sample. Since these voids are not modelled in the simulation, the numerical results would present better flexural strength in thermoplastic samples relative to thermosetting samples at some angles than the experimental results would. Therefore, it is reasonable to postulate that thermoplastic 3D woven composite could be superior at some angles in terms of flexural strength as compared to its thermosetting counterpart if air pockets within thermoplastic samples could be further minimised during fabrication process.

Second, the simulation model is formulated at macro-scale level instead of micro-scale level that could fully mimic the actual 3D woven composite. To avoid any confusion, modelling at micro-scale level means modelling the structure of fibre and matrix separately and combining them afterwards. Such model is identical to the actual sample in the sense that it shows distinctive fibre phase and matrix phase even if in combination. On the contrary, fibre and matrix would appear as a single structure if it is modelled at macro-scale level. In this case, composite is being modelled as a homogeneous structure throughout which the particles of fibre and matrix are evenly distributed. This has defied the anisotropic characteristics of composite for sure. The only aspect that makes macro-scale model anisotropic is the assigning of Young's modulus, shear modulus and Poisson's ratio along three axes and planes that describes the elastic behaviour of an anisotropic material. Therefore, macro-scale model would be slightly different in its mechanical behaviour as compared to the actual 3D woven composite.

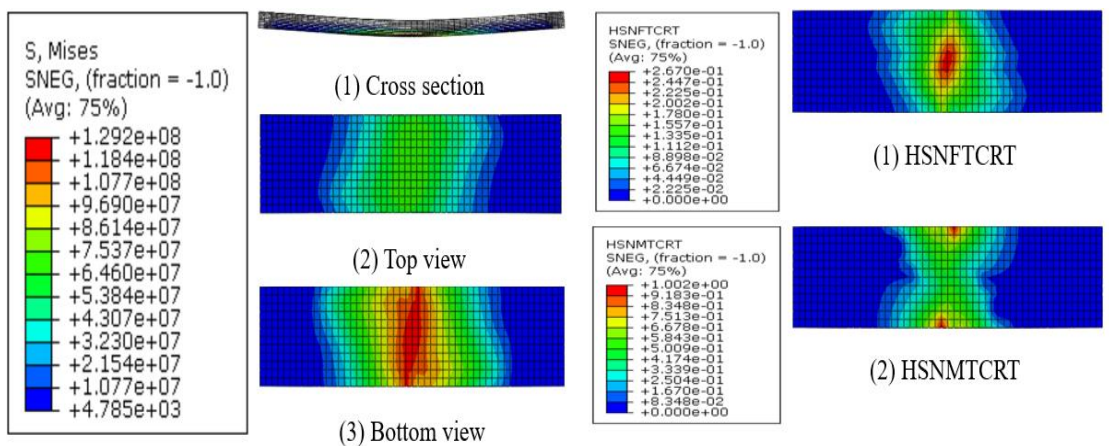
Despite having disparity between numerical and experimental results, the current study has produced a macro-scale model that could show the effect of off-axis angles on the flexural strength, the location of damage initiation, the area of damage and also the failure mode of both thermosetting and thermoplastic 3D woven composite. It could serve as a stepping stone for future work to work on micro-scale modelling in order to obtain flexural strength that is as closed to actual value as possible. More importantly, the current study could rekindle the interest of researching on thermoplastic composite by putting forth evidences of thermoplastic composite being a potential substitute to its thermosetting counterpart.



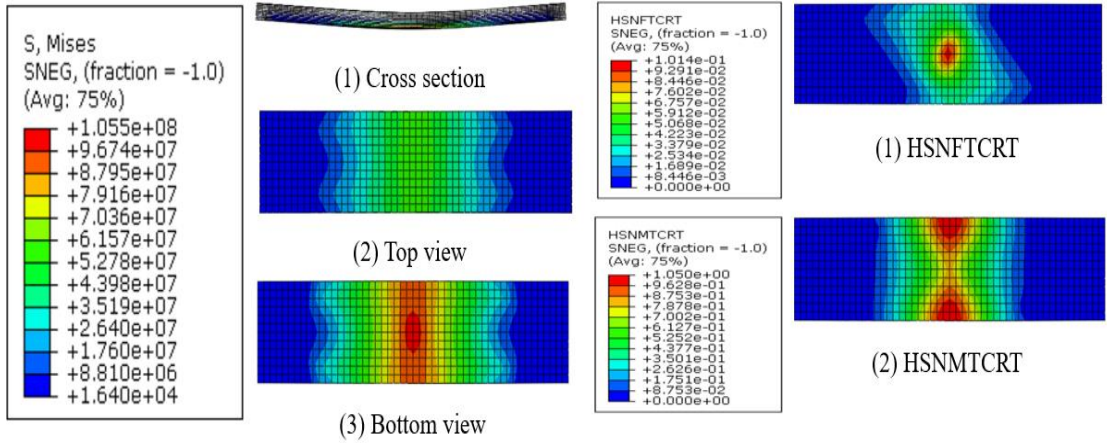
(a) Stress distribution throughout the specimen (b) Hashin damage criteria at the bottom of the specimen  
 Figure 4.8: Damage initiation of 0 degree thermosetting 3D woven composite



(a) Stress distribution throughout the specimen (b) Hashin damage criteria at the bottom of the specimen  
 Figure 4.9: Damage initiation of 15 degree thermosetting 3D woven composite



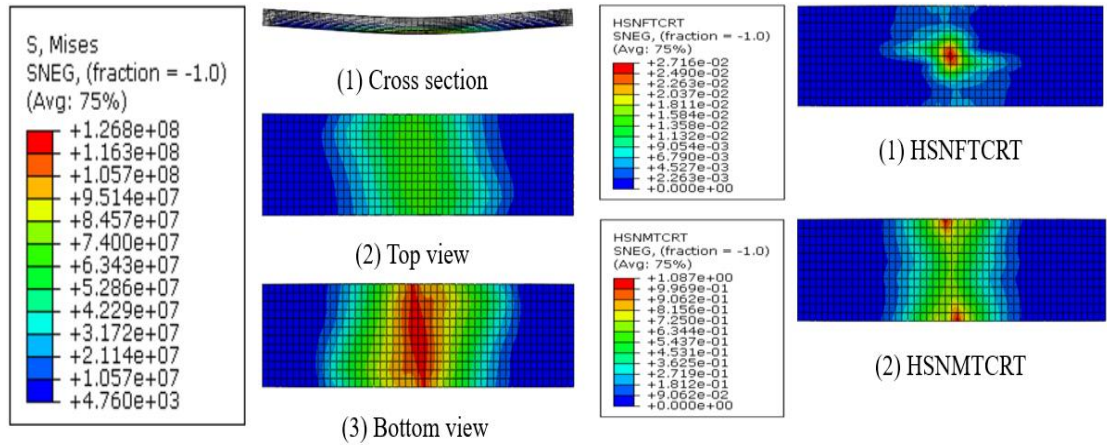
(a) Stress distribution throughout the specimen (b) Hashin damage criteria at the bottom of the specimen  
 Figure 4.10: Damage initiation of 30 degree thermosetting 3D woven composite



(a) Stress distribution throughout the specimen

(b) Hashin damage criteria at the bottom of the specimen

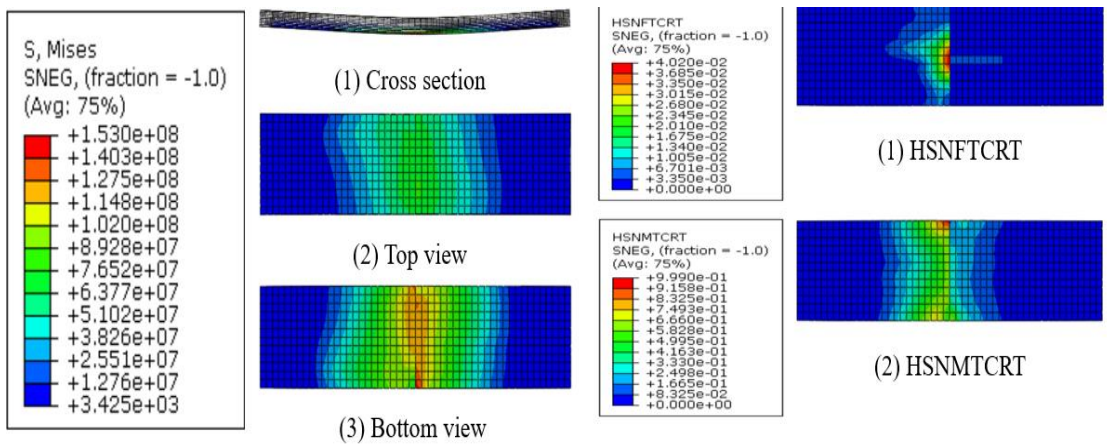
Figure 4.11: Damage initiation of 45 degree thermosetting 3D woven composite



(a) Stress distribution throughout the specimen

(b) Hashin damage criteria at the bottom of the specimen

Figure 4.12: Damage initiation of 60 degree thermosetting 3D woven composite

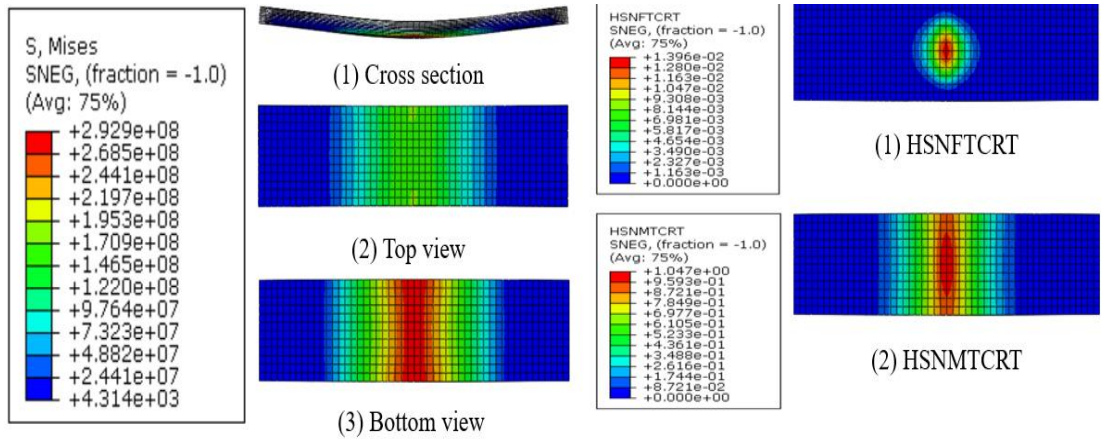


(a) Stress distribution throughout the specimen

(b) Hashin damage criteria at the bottom of the specimen

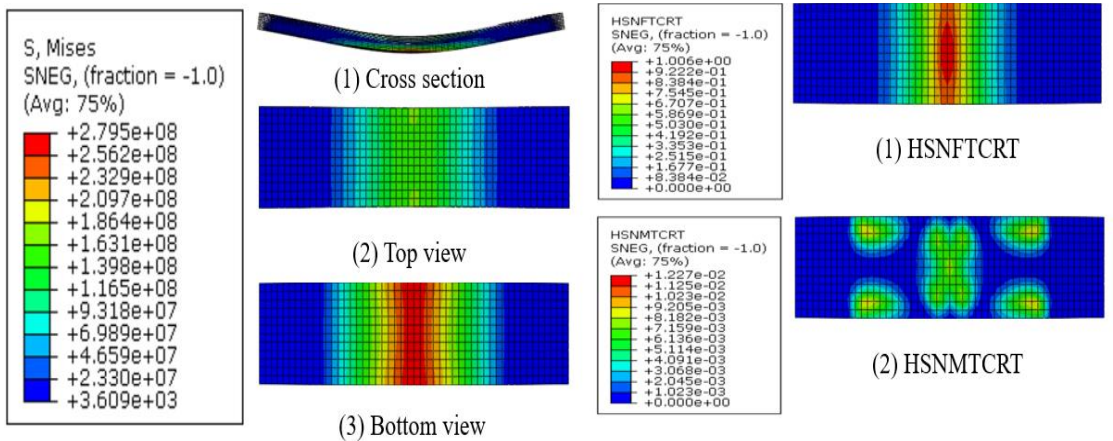
Figure 4.13: Damage initiation of 75 degree thermosetting 3D woven composite





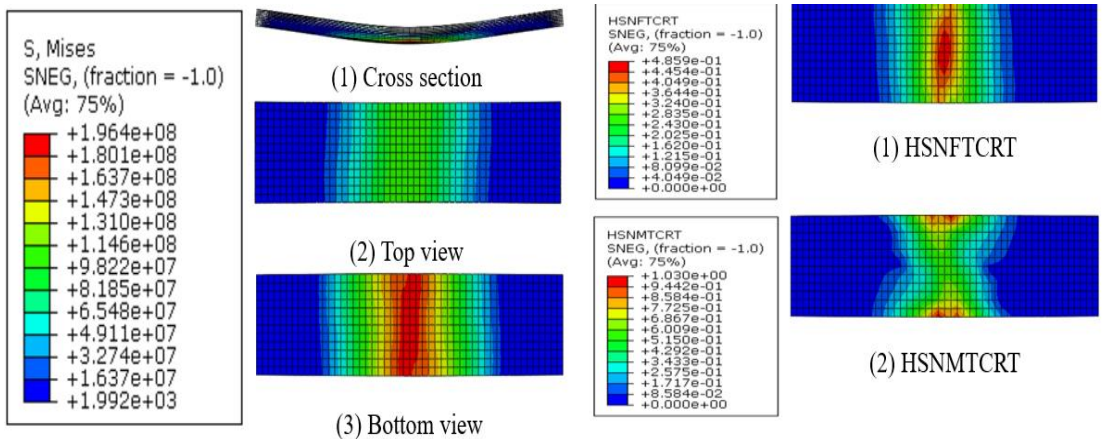
(a) Stress distribution throughout the specimen (b) Hashin damage criteria at the bottom of the specimen

Figure 4.14: Damage initiation of 90 degree thermosetting 3D woven composite



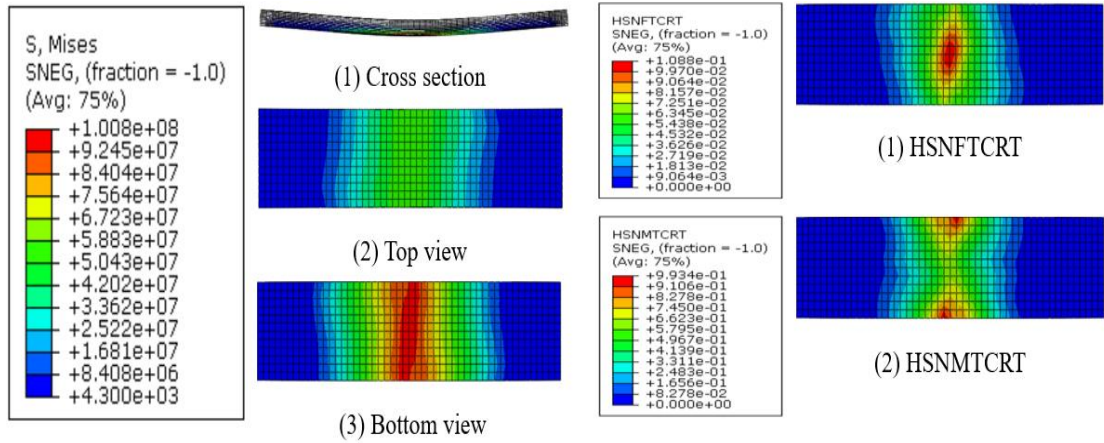
(a) Stress distribution throughout the specimen (b) Hashin damage criteria at the bottom of the specimen

Figure 4.15: Damage initiation of 0 degree thermoplastic 3D woven composite



(a) Stress distribution throughout the specimen (b) Hashin damage criteria at the bottom of the specimen

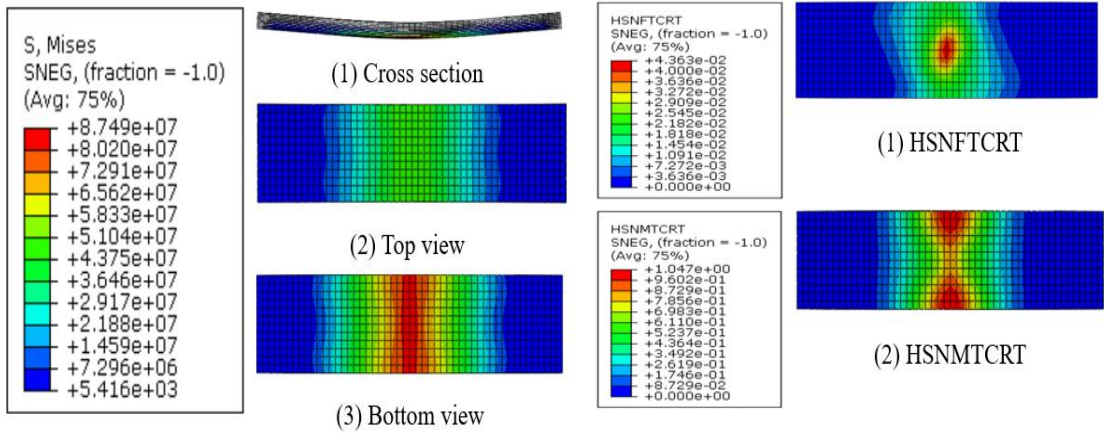
Figure 4.16: Damage initiation of 15 degree thermoplastic 3D woven composite



(a) Stress distribution throughout the specimen

(b) Hashin damage criteria at the bottom of the specimen

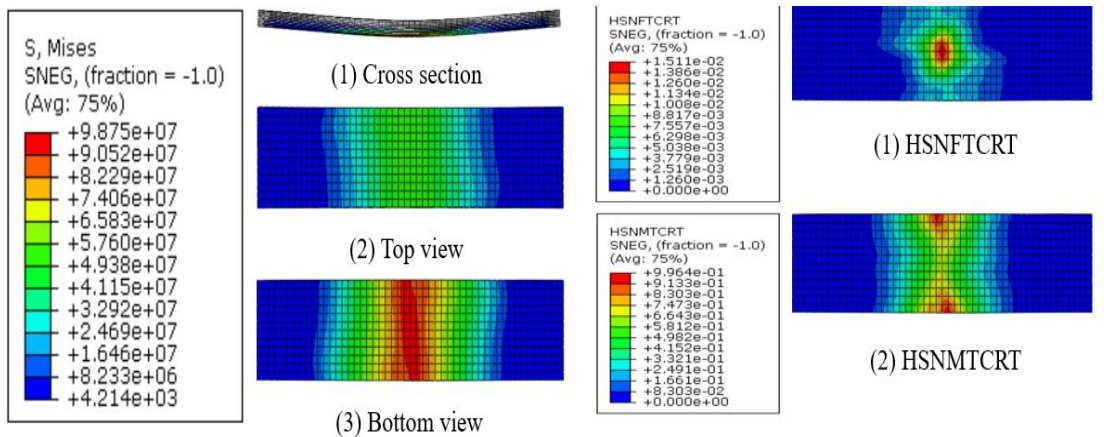
Figure 4.17: Damage initiation of 30 degree thermoplastic 3D woven composite



(a) Stress distribution throughout the specimen

(b) Hashin damage criteria at the bottom of the specimen

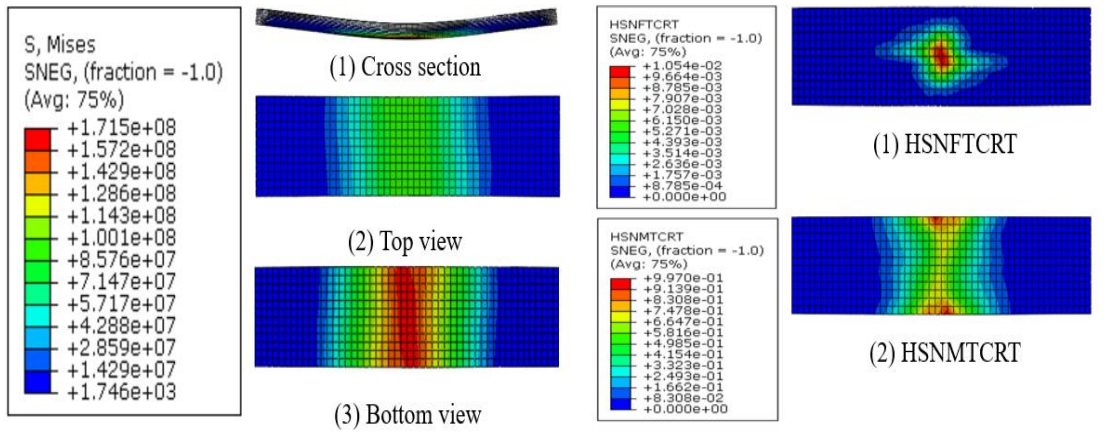
Figure 4.18: Damage initiation of 45 degree thermoplastic 3D woven composite



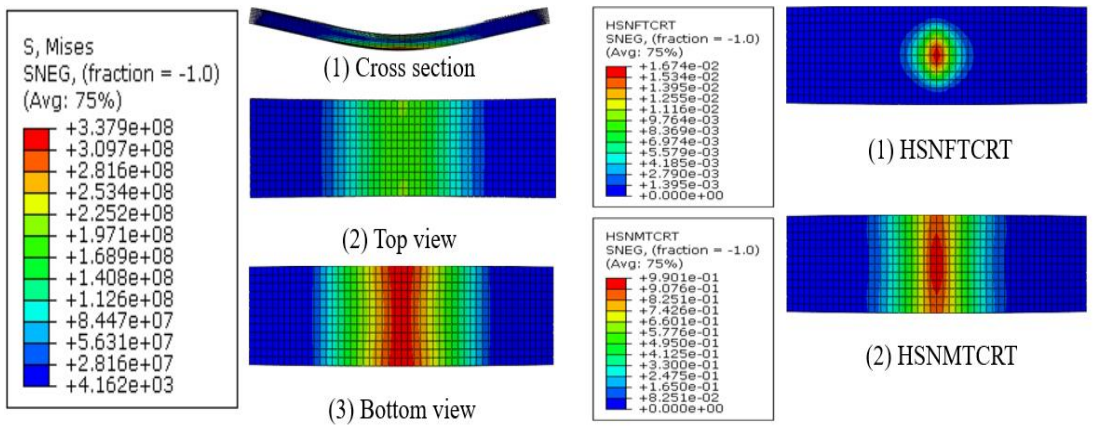
(a) Stress distribution throughout the specimen

(b) Hashin damage criteria at the bottom of the specimen

Figure 4.19: Damage initiation of 60 degree thermoplastic 3D woven composite



(a) Stress distribution throughout the specimen (b) Hashin damage criteria at the bottom of the specimen  
 Figure 4.20: Damage initiation of 75 degree thermoplastic 3D woven composite



(a) Stress distribution throughout the specimen (b) Hashin damage criteria at the bottom of the specimen  
 Figure 4.21: Damage initiation of 90 degree thermoplastic 3D woven composite

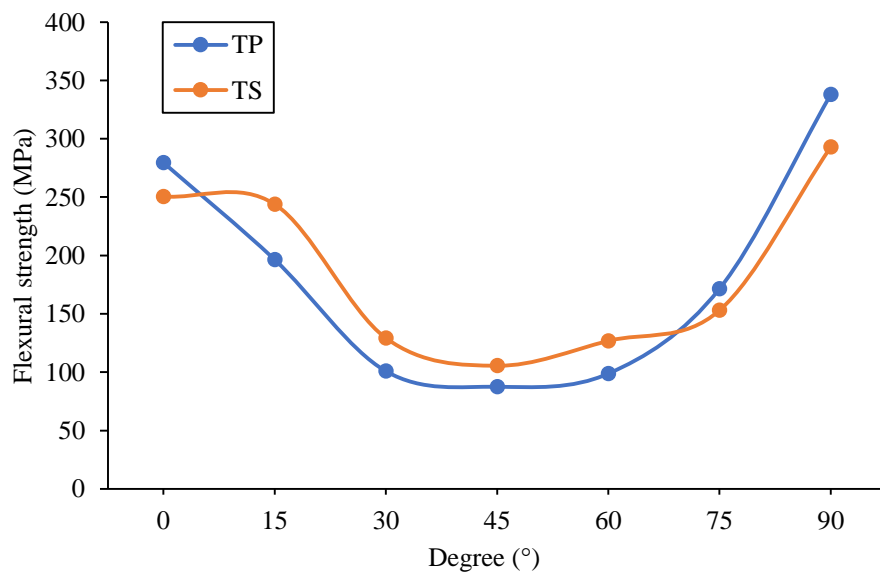


Figure 4.22: Comparison of thermoplastic and thermosetting specimens at different off-axis angles in terms of numerical flexural strength

Table 4.1: Comparison of experimental and numerical flexural strength

Resin	Off-axis angle (°)	Experimental flexural strength (MPa)	Numerical flexural strength (MPa)	Percentage of error (%)
Thermosetting	0	250.500	249.447	0.422
	45	105.500	162.401	35.037
	90	292.900	454.861	35.607
Thermoplastic	0	279.500	249.168	12.173
	45	87.490	135.410	35.389
	90	337.900	418.154	19.192

## **CHAPTER 5**

### **CONCLUSION AND RECOMMENDATION**

#### **5.1 Conclusion**

Answering to the issue of rife usage of thermosetting 3D composite in composite manufacturing industry, this paper has revealed the better quality of thermoplastic 3D woven composite in serving bending load related purpose. This makes it a potential surrogate for thermosetting 3D woven composite without compromising the mechanical performances of parts made of composite. This potential breakthrough is supported and proven by the following important findings in the current study.

- Compared to thermosetting samples, thermoplastic samples have flexural strains of about 13% higher. This means that precaution can be taken such as replacing a thermoplastic composite part under working condition when it reaches a safety threshold for bending deflection beyond which it is likely to fail. In the contrary, thermosetting composite part does not provide warning ahead of catastrophic failure as its sign of failure is not obvious.
- Compared to thermosetting samples, thermoplastic samples could absorb more energy per unit volume up to fracture, which is around 6.5% higher. This indicates that thermoplastic composite part is less prone to fracture given the same amount of energy is applied to both thermosetting and thermoplastic composite parts.
- Compared to 0 and 90 degree sample, 45 degree sample is superior in terms of flexural strain and energy absorption. Therefore, the advantage of 45 degree sample should be incorporated with that of thermoplastic sample to create stronger material.
- When being subject to flexural load, 45 degree thermoplastic sample exhibit the least amount of delamination among all kind of samples, making it the strongest material to withstand bending without suffering much damage. On a side note, delamination of 3D woven composite are shown by the development of white region around the mid span of sample.
- According to numerical analysis, the flexural strength of thermoplastic samples

could have been higher as compared to thermosetting samples at angles range from 0 to 5 degree and from 70 to 90 degree given that the forming of voids is kept at its minimal during post-curing process of composite.

## **5.2 Recommendation**

Recommendations for future work are summarised as follow.

- Forming of air pockets within thermoplastic composite should be reduced with proper method. Thermoplastic resin is highly volatile that it restricts vacuum resin infusion of thermoplastic composite from being carried out at high pressure to prevent forming of massive amount of bubbles. During post-curing process, highly volatile thermoplastic resin would evaporate due to exposure to atmospheric pressure, introducing voids to the structure of thermoplastic samples which jeopardise the structural integrity and thus reduce the flexural strength of that sample. As a result, a conventional thermoplastic composite has lower flexural strength as compared to thermosetting composite which barely forms any voids during post-curing.
- Modelling of composite at micro-scale level is more desirable as it is more likely to mimic the actual 3D woven composite. In the current study, the composite is modelled at macro-scale level and the percentage of error for numerical results is not satisfying enough to make it a valid model to predict the actual flexural strength of 3D woven composite. Micro-scale modelling is not attempted in the current study as it is way too complicated and is not possible to be completed within the allocated time frame.
- Micro-scale damage characterisation should be done using technique such as Scanning Microscope Electron (SEM), Computerized Tomography (CT) scan, optical microscopy and so on. This is to provide images of damage of internal structure which is not possible to be generated through visual inspection.

## REFERENCES

- [1] M.H. Mohamed and Z.-H. Zhang, "Method of Forming Variable Cross-Sectional Shaped Three-Dimensional Fabrics". US Patent 5085252, 4 February 1992.
- [2] Ince, M. E., (2013). Performance of composites from 3D orthogonal woven preforms in terms of architecture and sample location during resin infusion (Doctoral dissertation). Raleigh: North Carolina State University.
- [3] Ribeiro, M. C. S., Meira-Castro, A. C., Silva, F. G., Santos, J., Meixedo, J. P., Fiúza, A., ... & Alvim, M. R. (2015). Re-use assessment of thermoset composite wastes as aggregate and filler replacement for concrete-polymer composite materials: A case study regarding GFRP pultrusion wastes. *Resources, Conservation and Recycling*, 104, 417-426.
- [4] Dong, P. A. V., Azzaro-Pantel, C., & Cadene, A. L. (2018). Economic and environmental assessment of recovery and disposal pathways for CFRP waste management. *Resources, Conservation and Recycling*, 133, 63-75.
- [5] Hu, Q., Memon, H., Qiu, Y., & Wei, Y. (2019). The Failure Mechanism of Composite Stiffener Components Reinforced with 3D Woven Fabrics. *Materials*, 12(14), 2221.
- [6] F.C. Campbell. (2010). Structural Composite Materials. ASM International
- [7] Wang, Y., & Zhao, D. (2006). Effect of fabric structures on the mechanical properties of 3-D textile composites. *Journal of Industrial Textiles*, 35(3), 239-256.
- [8] Umer, R., Alhussein, H., Zhou, J., & Cantwell, W. J. (2017). The mechanical properties of 3D woven composites. *Journal of Composite Materials*, 51(12), 1703-1716.
- [9] Mountasir, A., Hoffmann, G., Cherif, C., Löser, M., & Großmann, K. (2015). Competitive manufacturing of 3D thermoplastic composite panels based on multi-layered woven structures for lightweight engineering. *Composite Structures*, 133, 415-424.
- [10] Zhang, D., Sun, M., Liu, X., Xiao, X., & Qian, K. (2019). Off-axis bending behaviors and failure characterization of 3D woven composites. *Composite Structures*, 208, 45-55.
- [11] Archer, E., Mulligan, R., Dixon, D., Buchanan, S., Stewart, G., & McIlhagger,

- A. T. (2012). An investigation into thermoplastic matrix 3D woven carbon fibre composites. *Journal of Reinforced Plastics and Composites*, 31(13), 863-873.
- [12] Behera, B. K., & Dash, B. P. (2014). An experimental investigation into the mechanical behaviour of 3D woven fabrics for structural composites. *Fibers and Polymers*, 15(9), 1950-1955.
- [13] Umair, M., Hamdani, S. T. A., Asghar, M. A., Hussain, T., Karahan, M., Nawab, Y., & Ali, M. (2018). Study of influence of interlocking patterns on the mechanical performance of 3D multilayer woven composites. *Journal of Reinforced Plastics and Composites*, 37(7), 429-440.
- [14] Yao, L., Rong, Q., Shan, Z., & Qiu, Y. (2013). Static and bending fatigue properties of ultra-thick 3D orthogonal woven composites. *Journal of composite materials*, 47(5), 569-577.
- [15] Nayak, S. Y., Shenoy, H. S., Rao, S. U., Narang, K., & Pant, K. V. (2015). Mechanical properties of multi layer plain weave and 3-D glass fabric epoxy composites. *International Journal of Composite Materials*, 5(2), 30-36.
- [16] Zhang, Q., Fang, X., Sun, X., Sun, B., & Qiu, Y. (2014). Comparison of the mechanical properties between 2D and 3D orthogonal woven ramie fiber reinforced polypropylene composites. *Polymers and Polymer Composites*, 22(2), 187-192.
- [17] Sun, F., Sun, Y., Zhang, Q., Zhang, D., & Chen, L. (2014). Experimental investigation on bending behavior of 3D non-crimp orthogonal composite. *Journal of Reinforced Plastics and Composites*, 33(20), 1869-1878.
- [18] Gao, X., Tao, N., Yang, X., Wang, C., & Xu, F. (2019). Quasi-static three-point bending and fatigue behavior of 3-D orthogonal woven composites. *Composites Part B: Engineering*, 159, 173-183.
- [19] Salviato M, Kirane K, Ashari SE, Bažant ZP, Cusatis G. Experimental and numerical investigation of intra-laminar energy dissipation and size effect in two-dimensional textile composites. *Compos Sci Technol* 2016;135:67–75.
- [20] Salviato M, Chau VT, Li WX, Bažant ZP, Cusatis G. Direct testing of gradual postpeak softening of fracture specimens of fiber composites stabilized by enhanced grip stiffness and mass. *J Appl Mech* 2016;83. 111003-1-10.



- [21] Liu G, Zhang L, Guo LC, Wang QM, Liao F. A modified V-notched beam test method for interlaminar shear behavior of 3D woven composites. *Compos Struct* 2017;181:46–57.